نموذج رقم (1)

إقـــــرار

أنا الموقع أدناه مقدم الرسالة التي تحمل العنوان:

STUDY OF SOME ELECTRIC, MAGNETIC AND DIELECTRIC PROPERTIES OF Ni-Zn SPINELS FERRITE

دراسة بعض الخواص الكهربية والمغناطيسية والعزل الكهربائي لمركب نيكل – زنك فريت

أقر بأن ما اشتملت عليه هذه الرسالة إنما هو نتاج جهدي الخاص، باستثناء ما تمت الإشارة إليه حيثما ورد، وإن هذه الرسالة ككل أو أي جزء منها لم يقدم من قبل لنيل درجة أو لقب علمي أو بحثي لدى أي مؤسسة تعليمية أو بحثية أخرى.

DECLARATION

The work provided in this thesis, unless otherwise referenced, is the researcher's own work, and has not been submitted elsewhere for any other degree or qualification

Student's name:	اسم الطالب: لبنى سهيل ابو عودة
Signature:	التوقيع:
Date:	التاريخ: 2015/12/9

Islamic University of Gaza
Research and Graduate Affairs
Faculty of Science
Department of Physics

STUDY OF SOME ELECTRIC, MAGNETIC AND DIELECTRIC PROPERTIES OF Ni-Zn SPINELS FERRITE

BY

Lubna Suhail Abu Ouda

Supervisor

Dr. Hussain Dawoud

Submitted to the Faculty of Science as a Partial Fulfillment of the Master Degree of Science (M. Sc.) in Physics

1436 – 2015

الرقم: ج س غ/35/   Ref ....

22/08/2015   Date .... التاريخ

نتيجة الحكم على أطروحة ماجستير

بناءً على موافقة شئون البحث العلمي والدراسات العليا بالجامعة الإسلامية بغزة على تشكيل لجنة الحكم على أطروحة الباحثة/ لبنــى ســهيل محمـــد أبوعــودة لنيــل درجـة الماجستير فـي كليـة *العلــوم* قسم الفيزياء وموضوعها:

دراسة بعض الخواص الكهربية والمغناطيسية والعزل الكهربائي لمركب نيكل – زنك فريت
Study of some Electric, Magnetic, and Dielectric Properties of Ni-Zn Spinels Ferrite

وبعد المناقشة العلنية التي تمت اليوم السبت 07 ذو القعدة 1436هـ، الموافق 2015/08/22م الساعة الحادية عشرة صباحاً ، اجتمعت لجنة الحكم على الأطروحة والمكونة من:

د. حسيـن عبدالكـريـم داود	مشرفاً ورئيساً	
د. سميـر سليمـان يـاسين	مناقشاً داخلياً	
د. محمد عبد الرؤوف رضوان	مناقشاً خارجيًا	

وبعد المداولة أوصت اللجنة بمنح الباحثة درجة الماجستير في كلية العلوم/ قسم الفيزياء.

واللجنــة إذ تمنحها هــذه الدرجــة فإنهــا توصـيهـا بتقــوى الله ولـزوم طاعتـه وأن تسخر علمها فـي خدمة دينها ووطنها.

والله ولي التوفيق ،،،

نائب الرئيس لشئون البحث العلمي والدراسات العليا

أ.د. عبدالرؤوف علي المناعمة

DEDICATION

To my father, mother, brothers, and sisters for their support, continuous encouragement, and love.

Acknowledgements

No words can ever express my sincere gratitude to Allah who granted me the strength, support and eased the difficulties, which I faced during the accomplishment of this thesis

I would like to express my deep thanks to my supervisor, ***Dr. Hussain Dawoud,*** who has supported me throughout my thesis with his patience and knowledge. I attribute the level of my Master's degree to his encouragement and effort and without him this thesis, too, would not have been completed or written.

 In addition, I would like to thank all the staff members of physics department in the Islamic University; indeed they extended a helping hand wherever I asked them to.
I would like to thank everyone who gave advice or assistance that contributed to complete this research

Finally, and perhaps most importantly I would like to thank my family for their unwavering support .

ABSTRACT

In the present work FT- IR spectra , magnetic properties , dc conductivity, the dielectric constant and the dielectric loss tangent are investigated at room temperature and elevated temperatures.

Experimentally the mixed ferrite $Ni_{1-x}Zn_xFe_2O_4$ (where x=0.0, 0.2, 0.4, 0.6, 0.8 and 1) were prepared from high purity oxides using standard ceramic technique. The FT- IR spectra in the range from 350 to 1000 cm^{-1} were reported. Mainly ,two bands were observed. The first band at around 400 cm^{-1} v_O and the second band at around (600-550cm^{-1}) v_T were assigned to the octahedral and tetrahedral complexes, respectively.

Furthermore , The magnetization M was measured at room temperature in the range of magnetizing field H from 0 up to 3500Am^{-1} .The results indicated that the increasing of the magnetization as Zn^{2+} ions increased for samples of x≤ 0.6 while the magnetization of the samples of x ≥ 0.8 decresed when Zn^{2+} ion increased.

The conductivity was measured as a function of temperature and the relation between $ln\sigma$ $(\Omega.cm)^{-1}$ with temperature indicate that the conductivity is increased with temperature which revel that the samples under investigation has a semiconductor behavior . Also from the relation between $ln(\sigma T)$ and temperature showed that there are two different slops , this change of slope is attributed to the change of samples from ferrimagnetic to paramagnetic "curie point" .And its found that the curie point decrease as Zn^{2+} increased .

To determine the Curie point, the inductance was measured as a function of temperature for the above investigated ferrite. The inductance seems to be constant till curie point temperature T_c , at this temperature T(K) the inductance decreases sharply. Tc was also found to decrease with increasing the Zn^{2+} ions .

Dielectric properties such as dielectric constant ε, and the dielectric loss tangent tan (δ) has been investigated in the range of frequency $(10^4-10^6)Hz$ at room temperature. It was found that the value of ε and tan (δ) decrease continuously with increasing frequency , this is attributed to the mechanism of polarization process in the ferrite which is similar to that of the conduction process.

ARABIC SUMMARY

الملخص العربي

فى هذا البحث سيتم دراسة الاشعة تحت الحمراء ، الخواص المغناطيسية ، التوصيلة الكهربائية فى حالة التيار المستمر و ثابت العازلية عند درجة حرارة الغرفة ودرجات حرارة مختلفة.

تم تحضير مركب زنك – نيكل فريت حسب الصيغة $(Ni_{1-x}Zn_xFe_2O_4)$ حيث $(x= 0.0, 0.2, 0.4, 0.6, 0.8, \&1)$ من أكاسيد عالية النقاء باستخدام الطريقة السيراميكية القياسية

تم دراسة طيف الاشعة تحت الحمراء في المدى (350 to 1000cm^{-1}) حيث ظهر وجود منطقتان رئيسيتان من مناطق الامتصاص الاول حول ($\nu_0= 400$ cm^{-1}) وهى ترمز الى الموقع الثماني (B-site) والثانية حول ($\nu_T = 600\text{-}550$cm^{-1}) وهى ترمز الى الموقع الرباعي (A-site).

علاوة على ذلك. تم قياس المغناطيسية (M) عند درجة حرارة الغرفة في المجال المغناطيسي المتغير من (0 to 3500Am^{-1}) واوضحت النتائج ان المغناطيسية تزداد بزيادة تركيز أيونات Zn^{2+} في العينات حتى ($x \leq 0.6$) ، بينما تقل المغناطيسية بزيادة تركيز أيونات Zn^{2+} في العينات حتى ($x \geq 0.8$) .

قيست الموصلية الكهربية كدالة في درجة الحرارة، ومن العلاقة بين (lnσ) و(درجة الحرارة) تبين ان الموصلية تزداد بزيادة درجة الحرارة وهذا يحقق ان العينات لها خواص أشباه الموصلات. أيضا العلاقة بين (درجة الحرارة) و (lnσT) أظهرت تغير في ميل المماس ، هذا التغير في المماس بسبب تغير وانتقال العينة من حالة ferrimagnetic الى حالة paramagnetic هذه الدرجة تسمى درجة كوري ، والتي وجد أنها تقل بزيادة تركيز أيونات Zn^{2+} .

لقياس درجة كوري تم قياس معامل الحث كدالة في درجة الحرارة لمركب الفرايت المذكور حيث وجد ان معامل الحث يكون ثابت حتى درجة حرارة معينة وهي درجة كوري والتي عندها يحدث نقص حاد في قيمة معامل الحث . ووجد ان درجة كوري تقل بزيادة تركيز أيونات الزنك .

تم حساب خصائص العازلية مثل ثابت العزل(ε) dielectric constant ، وثابت الفقد (tan δ) dielectric loss tangent في مدى ترددي $Hz(10^6 - 10^4)$ في درجة حرارة الغرفة ، وقد وجد ان قيمة (ε) , (tan δ) تقل بزيادة التردد ، وهذا يعزى إلى أن آلية عملية الاستقطاب في الفرايت مماثلة لتلك العملية في التوصيل.

LIST OF FIGURES

LIST OF TABLES

CONTENTS

CHAPTER I : THEORETICAL REVIEW

CHAPTER II : LITERATURE SURVEY

CHAPTER III: EXPERIMENTAL TECHNIQUES AND APPARATUS

CHAPTER IV : RESULTS AND DISCUSSION

CHAPTER I

THEORETICAL REVIEW

1-1INTRODUCTION

The origin of the magnetism lies in the orbital and the spin motion of the electrons and how the electrons interact with each other. The best way to introduce the different types of the magnetism is to describe how the material responds to the applied magnetic field.

Materials are called magnetic materials when they are magnetized by the magnetic field. The intensity of the intrinsic magnetization of the magnetic substance M is defined as the magnetic moment $\boldsymbol{\mu_m}$ per unit volume of the magnetic substance [1].These materials are classified according to their magnetic susceptibility χ_m values that change with the applied magnetic field intensity as well as temperature. There are various kinds of the magnetic materials. The magnetic behavior of the magnetic materials can be classified into five major groups diamagnetic, paramagnetic, ferromagnetic, antiferromagnetic and ferromagnetic [2]. These groups are illustrated in figure (I).

1-2 Types of magnetic materials
1-2-1 Diamagnetism

Diamagnetism is described for the materials which have a very weak magnetism in which their magnetization M acts in the opposite direction of the applied magnetic field H. The origin of this magnetism is the orbital rotation of the electrons about their nuclei which are induced electromagnetically by the application of an external field .They are composed of the atoms which have no net magnetic moment. However, when they expose to an external field a negative magnetization is produced and thus; the magnetic susceptibility is negative.

1-2-2 Paramagnetism

Paramagnetism is described for the materials which contain some atoms or ions with a net magnetic moment due to unpaired electrons, and from the

realignment of the electron paths caused by the external magnetic field. Paramagnetic materials have a small, positive susceptibility to magnetic fields. These materials are slightly attracted by a magnetic field and the material does not retain the magnetic properties when the external field is removed.

1-2-3 Ferromagnetism

Ferromagnetism is described for the materials which their spins are aligned parallel to each other. Ferromagnetism materials have a large, positive susceptibility to an external magnetic field. They exhibit a strong attraction to magnetic fields and are able to retain their magnetic properties after the external field has been removed. Ferromagnetic materials have some unpaired electrons so their atoms have a net magnetic moment. They get their strong magnetic properties due to the presence of magnetic domains .

1-2-4 Antiferromagnetism

Antiferromagnetism is described for the materials which have a weak magnetism. This is similar to the paramagnetic materials in the sense of exhibiting a small magnetic susceptibility. The simplest model structure of these materials consists of two magnetic sublattices with the same magnetic moments, thus; their net magnet moment is zero. The individual magnetic moments on each sublattice are aligned ferromagnetically with antiparallel coupling between the two magnetic sublattices. Above a critical temperature, called Neel's temperature point T_N, thermal energy is sufficient to disorder the individual magnetic moments in antiferromagnetic materials which become paramagnetic.

1-2-5 Ferrimagnetism

The common example for the ferrimagnetic materials was considered that, these materials are divided into two magnetic sublattices, these materials are, considered as a class of the ferromagnetic and the antiferromagnetic materials.

The structure of the ferrimagnetic materials is composed of more than two magnetic sublattices which are separated by oxygen ions. Therefore, the exchange

interactions are mediated by the anions (oxygen, O^{2-} ions). When this happens, the interactions are called indirect or superexchange interactions.

The strongest interactions tend to an antiparallel alignment of the spins between the two sublattices. In these materials, the magnetic moments for the two sublattices are not the same, so the net magnetization of these materials is not zero. Their magnetic moments disappear above Curie temperature point T_c at which the thermal energy randomizes the individual magnetic moments and then these materials become paramagnetic. Thus; these materials have a spontaneous magnetization that arises from the nonparallel arrangements of the strong coupled atomic dipoles below a certain temperature. The color of this material varies from silver gray to black.

1-3 Aim of this Study

The mixed *Ni-Zn* spinel ferrite is soft ferrite. It has become more attractive material for microwave applications such as high quality filters, rod antenna, radio frequency circuits, transformer cores, read, write heads for high speed digital tape, isolators, circulators, gyrators, phase shifters, low-frequency inductors in deflection system in TV circuits, switch mode power supply, operating devices and telecommunication industry.

The aim of this work is to investigate the effect of diamagnetic element Zn^{2+} ions on the structure, the magnetic, the electric and the dielectric properties of *Ni Fe$_2$O$_4$*. The mixed *Ni -Zn* spinel ferrite were prepared using the standard ceramic method in the form of $Ni_{1-x} Zn_x F_2O_4$, where *x* stepped by 0.2 according to 0.0$\leq$ *x*$\leq$1.0. FT-IR absorption, *AC* and *DC* circuits are used to study; magnetic, electric and the dielectric properties of the above-mentioned compositions.
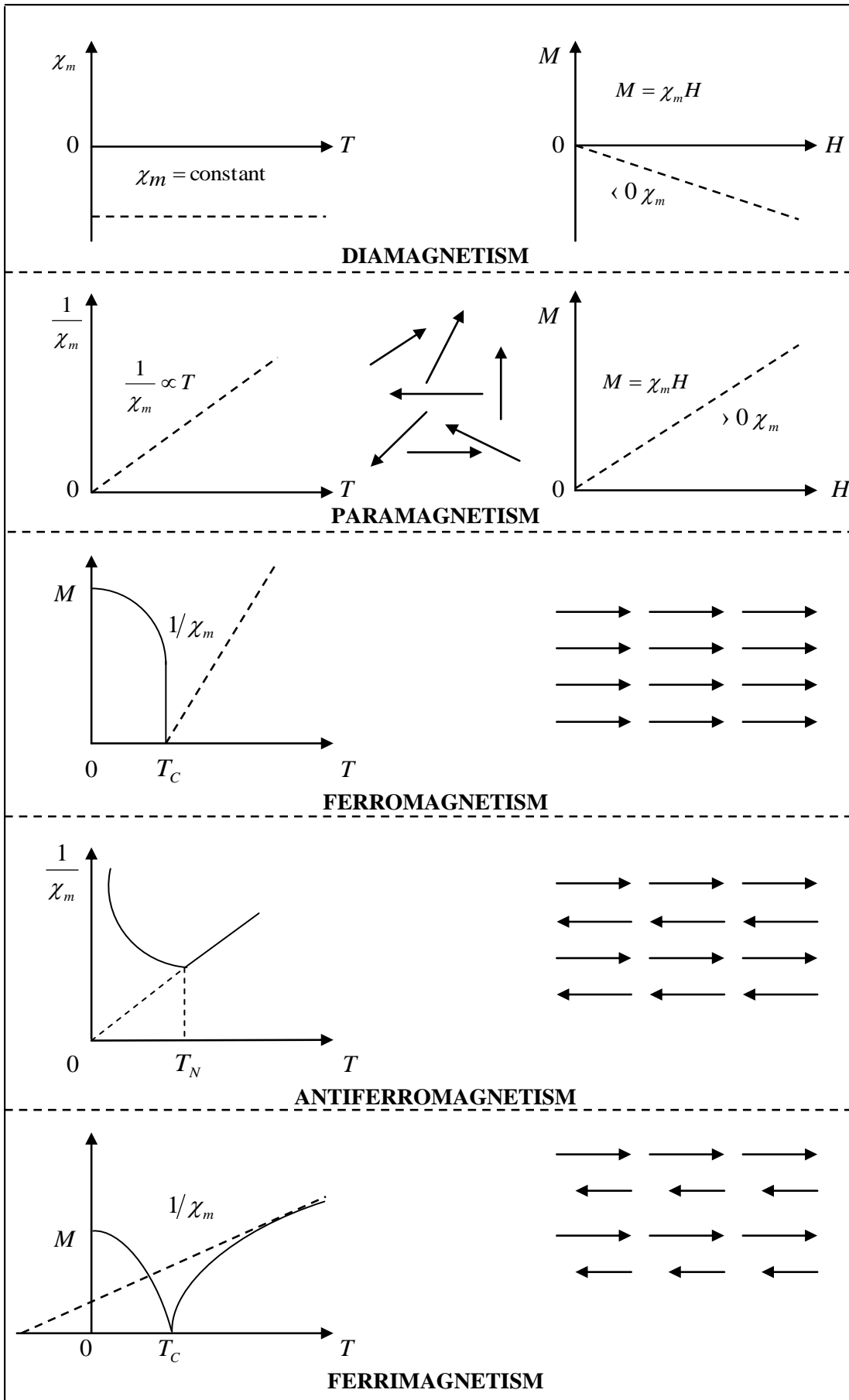
Fig. (I): Classification of the magnetic materials.

1-4 Applications of the Ferrimagnetic Materials

Ferrimagnetic materials are a class of ceramic materials with widely useful electromagnetic properties and interesting applications. The magnetite" lodestone" was the earliest application of these materials, which was used by the navigators to locate the magnetic North

Ferrimagnetic materials have become available as practical magnetic materials and have a number of important scientific and technological applications. This may be attributed to [3]

i. They have relativity large saturation magnetization.

ii. Their resistivities ranged between $10^2 \Omega.cm$ to $10^{13} \Omega.cm$.

iii. They are poor conductors of the electricity, specially, at room temperature.

These properties are valuable in the high frequency application, where the eddy current in the conducting materials poses problems.

1- 5 Types of the Ferrimagnetic Materials

Ferrimagnetic materials are made of iron oxides mixed with some other oxides. Therefore, there are many compounds of these materials which classified by a term descriptive of their crystal structure. These types are [4]

i. Ferrimagnetic spinel materials in the form *MeFe$_2$O$_4$* , where *Me* is a divalent metal atom of the same type, which may be either magnetic or non-magnetic, such as *Ni, Zn, Cu, Fe, Co, Mn, Mg* or *Cd* , e.g. nickel ferrite *NiFe$_2$O$_4$* and zinc ferrite *ZnFe$_2$O$_4$* , and , also, their combination, e.g. the mixed *Ni- Zn* spinel ferrite.

ii. Hexagonal oxides in the form *MeFe$_{12}$O$_{19}$*, where *Me* is a divalent metal atom of the same type, which may be either magnetic or non-magnetic, such as *Ba, Sr*, *Pb* and their combination, e.g. barium ferrite *BaFe$_{12}$O$_{19}$*.

iii. Ferrimagnetic garnet materials in the form *U$_3$Fe$_5$O$_{12}$* , where *U* is replaced by the trivalent rare earth ions, such as *Y, Pm, Sm, Eu, Gd, Tb, Dy, Ho, Er, Tm*, *Yb* or *Lu*. The rare earth garnets are commonly called RIG's. The commonly example for these materials is yttrium iron garnets YIG's in the

form $Y_3Fe_5O_{12}$. Other example for these materials is gadolinium iron garnets GdIG's.

Ferrimagnetic materials of ferrites have become available as practical magnetic materials. They are divided into four groups for applications, which are described in [5] as:

i- Hard Ferrites (Permanent Magnets)

Materials used for this application are barium ferrite $BaFe_{12}O_{19}$ and strontium ferrite $SrFe_{12}O_{19}$. These are hexagonal ferrite with a crystal structure of magneto–plumbite $pbFe_{12}O_{19}$. These materials are characterized by a high value of the uniaxial anisotropy field and a high coercive force. In addition, their resistivity is high, typically $10^8\,\Omega.cm$. The high coercive force allows these materials to be used as focusing magnets for television tubes, where there are strong demagnetization field. The high resistivity permits their use as permanent magnets where there is additional alternating high frequency magnetic flux without eddy current losses [6, 7].

ii-Soft Ferrites

The applications under this heading account for a major use of the ferrite materials. They include inductor cores, transformer cores, particularly line output transformers in television sets and rod aerials.

The essential requirement is materials with high permeability, low coercive force, low eddy current losses and the ability to operate up to frequencies of $10\,MHz$ with special requirements extending to $1000\,MHz$.

The initial permeability of the manganese and the nickel ferrite is rather low, about 250 (H·m^{-1}) and 10 (H·m^{-1}), respectively. If these materials are combined with zinc, the anisotropy is lowered and the permeability increases to about 1000 (H·m^{-1}) for the mixed *Mn-Zn* ferrite and 700 (H·m^{-1}) for the mixed *Ni-Zn* ferrite. The latter has the higher resistivity and lower losses [8].

iii-Rectangular Loop Ferrites

Rectangular Loop Ferrites are ferrites which have a rectangular hysteresis loop. This property makes them suitable for use in a magnetic memory core. Ferrite

communities used for this application are the mixed *Mn–Mg* ferrite and the mixed *Li-Ni* ferrite [9, 10].

iv-Microwave Ferrites

The processing of electromagnetic waves which is done in the frequency range from 1GHz to 100GHz are applications of Microwave Ferrites. This processing depends on the interaction of the electromagnetic waves with the processing spin moments in the ferrites. The discussion is restricted to one of the most important of those processes known as Faraday rotation. This is the rotation of the plane of polarization of a plane electromagnetic wave as it travels through the ferrites in the direction of the applied magnetic field. The most application of the Faraday rotation is to use waveguide just as one uses polarizer and analyzer in optics to accept are reject plane polarized wave. The most important microwave ferrites are manganese ferrite, nickel ferrite, cobalt ferrite and the mixed *Ni–Mn* ferrite [11].

1-6 Structure of Spinel Ferrite Materials

Ferrimagnetic spinel ferrites are the most common compound of the ferrimagnetic materials. The concept of the simplest structure of the ferrimagnetic spinel materials was explained to include two magnetic sublattices. The structure of the ferrite affects the physical properties of these ferrite.

1-6-1 Spinel Lattice Structure

Ferrimagnetic compound with cubic spinel structure have composition AB_2Z_4. The anions Z are replaced by the Oxygen atoms, i.e. O^{2-} ions , form the cubic closed-packed lattice. As shown in figure (1-1a)، A ions fill the tetrahedral interstices, i.e. T_d sites, and B ions fill the octahedral interstices, i.e. O_h sites, of the cations packing [12]. Figure (1-1a)، also، shows two units of AB_2Z_4 in a quarter of the unit cell. The lattice constant"a" for these materials varies with the compositions، it is about $8.5A^o$. Figure (1-1b) shows an isolated Z^{2-} ion with its nearest neighbors of the **A** and **B** ions [5]. The smallest cell of the spinel lattice structure that has cubic symmetry contains eight molecules of AB_2Z_4. Where the oxygen atoms have a fixed position, which have an ionic radius of about 1.32 A°

.This is larger than of the ionic radius of the metal ions, which varies between 0.6 A° to 0.8 A° [2]. This tends that, the metal ions occupy the interstitial position sites of the spinel lattice structure, which can be classified into two groups [5]

i. The T_d sites interstices are filled by the **A** ions, which have the ionic charge **p** and surround by four O^{2-} ions. They are represented by the bracket ( ).

ii. The O_h sites interstices are filled by the **B** ions, which have the ionic charge **q** and surround by six O^{2-} ions. They are represented by the bracket { }.

In the spinel lattice structure, the anions have a negative charge equal (**-8**), which comes from the four O^{2-} ions. Therefore, the total sum of the ionic charge of the cations, i.e. **p** and **q**, should be equal (+8). There are various possibilities of the ionic charge distribution of the cations of the spinel lattice structure which depend on the **A** and the **B** ions, while the cubic closed- packed lattice of the material is the same. The various possibilities of **p** and **q** values were listed in table (1-1) [13].

The common type of the spinel lattice structure is (2-3) spinel type, which have the highest electrostatic stability in the normal cations arrangement [14].

Hence, the **A** and the **B** ions have various distributions, this makes a change in some of the physical properties of these materials.

The simplest example for the ferrimagnetic spinel materials are the spinel iron, e.g. magnetite (magnetic oxide of iron) in the form ($Fe_1^{2+}Fe_2^{3+}O_4^{2-}$). Several mixed spinel ferrites can be produced by adding different oxides to the iron oxides, which give useful physical properties for several applications.
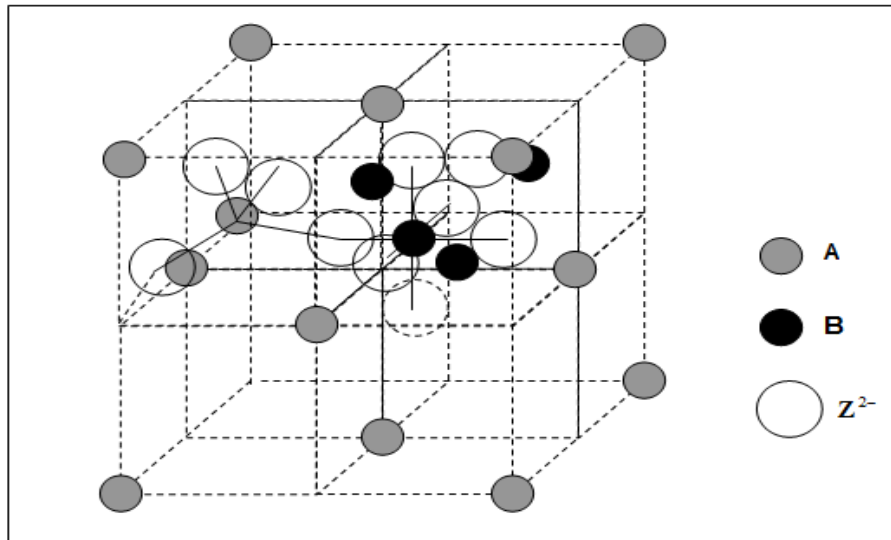
Fig. (1-1a): Two octants of the unit cell of the spinel lattice structure. A ions are at T_d sites and B ions are at O_h sites of the Z^{2-} anions packing.
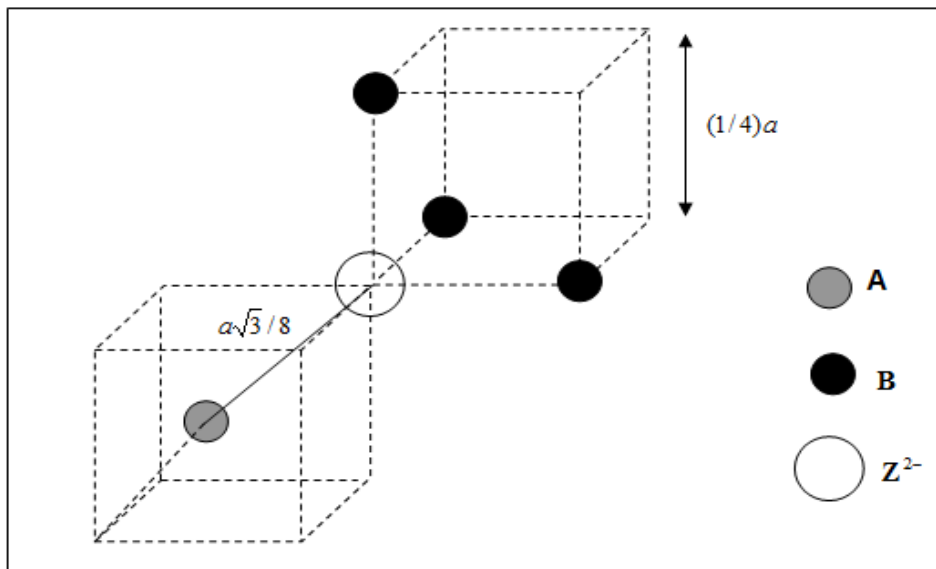
Fig. (1-1b): An anion Z^{2-} in the spinel lattice structure with it's nearest cations neighbors.

Table (1-1): Various possibilities of the ionic charge distribution of the cations of the spinel lattice structure.

Ionic charge value		Ionic Charge Distribution of Spinel Lattice	Type of Spinel Materials
p	q		
2	3	$(A_1^{2+})\{B_2^{3+}\}Z_4^{2-}$	(2-3) Spinel Type.
4	2	$(A_1^{4+})\{B_2^{2+}\}Z_4^{2-}$	(4-2) Spinel Type.
3	5/2	$(A_1^{3+})\{B_2^{(5/2)+}\}Z_4^{2-}$	(3-5/2) Spinel Type.
6	1	$(A_1^{6+})\{B_2^{1+}\}Z_4^{2-}$	(6-1) Spinel Type.

1-6-2 Types of Spinel Lattice Structure

The distribution of the metal ions at the T_d sites and the O_h sites is very important to understand the physical properties of the ferrimagnetic materials. More than one type of this distribution is found at the two sites for the materials in the form $MeFe_2O_4$. These types are described in Ref [5] as:

i.   Normal Spinel Structure

In this type, all the Me^{2+} divalent metal ions are found on the T_d sites and the Fe^{3+} trivalent iron ions appear only on the O_h sites. The formula of this type is found in the form

$$(Me^{2+})\{Fe_2^{3+}\}O_4^{2-}$$

ii.   inverse Spinel Structure

In this type, all the Me^{2+} divalent metal ions are found on the O_h sites. and Fe^{3+} trivalent iron ions are distributed in equal numbers over T_d sites and the O_h sites . The formula of this type is found in the form

$$(Fe^{3+})\{Me^{2+}Fe^{3+}\}O_4^{2-}$$
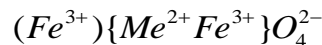
iii. Intermediate Spinel Structure

In the intermediate spinel structure the divalent metal ions Me^{2+} and the trivalent iron ions Fe^{3+} are distributed on the T_d sites and on the O_h sites. The formula of this type is found in the form

$$(Fe^{3+}_{1+x} \, Me^{2+}_{1-x}) \, \{ \, Me^{2+}_x Fe^{3+}_{1-x} \} \, O^{2-}_4$$
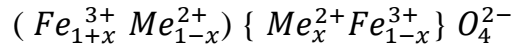
1-6-3 Factors Affecting on the Spinel Lattice Distribution

There are some factors that affect the distribution of the metal ions over the T_d sites and the O_h sites, such as the preparation method of the ferrimagnetic spinel compositions. Other effective factors are found in Ref [6]

i. Electrons Configuration

Matching of the electron configuration of the metal ion which surrounded by the O^{2+} ions. From the point of view of the valances, it seems reasonable to have the Me^{2+} ions at the T_d sites and the Fe^{3+} ions at the O_h sites. This is due to the number of the O^{2+} ions which are surrounded the T_d sites and the O_h sites by the ratio 4: 6, or 2 : 3, that corresponds to (2-3) spinel type.

This type corresponds to the *Zn* and the *Cd* spinel ferrite which are known as the normal spinel ferrite, where their ions have a special preference for a certain environment for the T_d sites, e.g. *Zn* $(4s^2 \, 3d^{10})$ and *Cd* $(5s^2 \, 4d^{10})$, and their electrons can form a covalent bond with the six (2p) electrons of the O^{2+} ions.

ii. Ionic Radius

According to the O^{2-} ions distribution on the spinel lattice, it can be evaluated that, the T_d sites are smaller than the O_h sites. Therefore, one might expect that, the smaller ions would prefer to occupy the T_d sites; however, the trivalent ions are smaller than the divalent ions, so this tends to favours the inverse spinel structure .

iii.   **Electrostatic (Madelung) Energy**

This is the electrostatic energy gained when the infinite ions are brought together to form the spinel lattice. In the normal arrangement, the metal ions with the smallest positive charge are surrounded by four O^{2+} ions, but the others metal ions with the higher positive charge, basically, Fe^{3+} ions, are surrounded by six O^{2+} ions. This is the most electrostatic favorable. In the ionic crystals, the ions arrange themselves in whatever crystal structure which gives the strongest attractive interactions compatible with the repulsive interactions at short distances between the ions core. The main contribution to the binding energy of the ionic crystals is the electrostatic energy which is called the Madelung energy [15].

1-7 Magnetic Properties of the Ferrimagnetic Materials

The electromagnetic properties of spinel ferrite depend on the chemical composition, the cations distribution and the method of preparation of samples [16].

The intensity of the intrinsic magnetization of the ferrimagnetic spinel materials can be explained according to the spins distribution of the magnetic ions at the T_d sites and the magnetic ions at the O_h sites that shown in figure (1-2) [5]. Noting that, in the ionic crystal, it is difficult to calculate the orbital magnetic moments [17]. So, the magnetization of these materials may be explained by the spin configurations. It arises usually from the spin magnetic moments of the unfilled shells 3d, for the transition elements, where the superexchange interaction between the sublattices and the six-2p oxygen electrons occurred. Such that an alignment of spins should be expected from the nature of the superexchange interactions. The superexchange interactions between the two cations; via an intermediate O^{2+} ions are greatest, if the three ions are colinear and their separations are not too large. The ions arrangement in the spinel lattice is likely to be most important as is shown in figure (1-3a throught e) [4, 6]. For the situation depicted in figure (1-3a) both the angle φ and the distance between the ion cores are favorable for superexchange interactions. For all the other cases, either the angle of figure (1-3c) or the distance of figures (1-3b and 1-3d), or both figure (1-3e) are unfavorable. The conclusion is

that the interactions between the sublattices are stronger than those within them. Further, these interactions between the ions within the T_d sites are the weakest of all. This result thus; supports the assumption that the sublattices magnetizations are antiparallel.
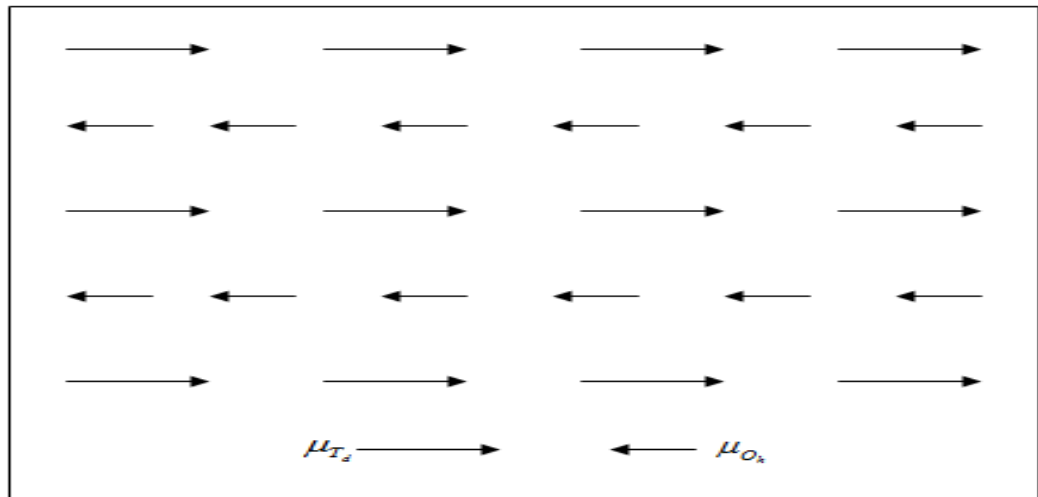
Fig. (1-2): Spins distribution at the T_d sites and the O_h sites.
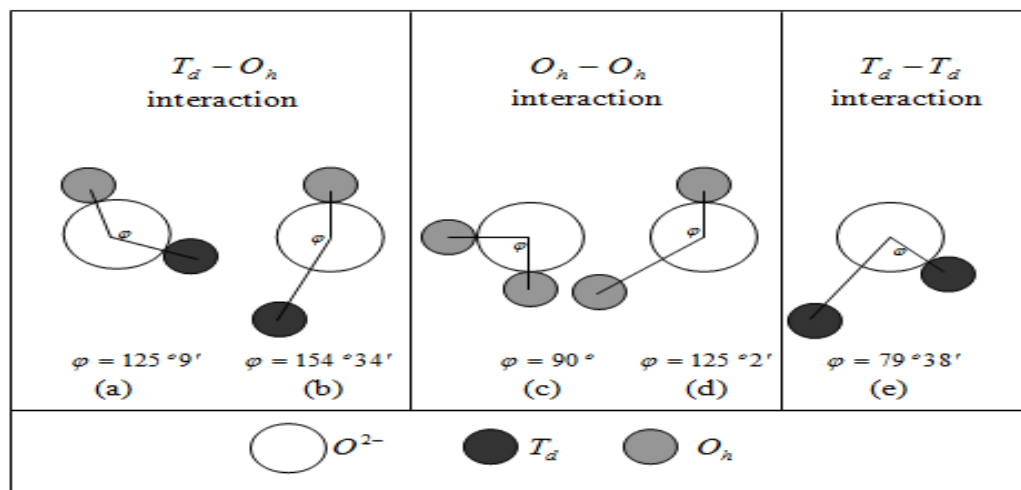
Fig.(1-3): Superexchange interactions between the anions, O^{2-} ions, and the cations, the T_d sites and the O_h sites.

1-7-1 Magnetization Process of the Ferrimagnetic Materials

The most important magnetic materials for practical proposed are the ferrimagnetic materials, because the best-known members iron, cobalt, nickel and the rare elements gadoliniums are found in the ferrimagnetic materials. The outstanding fact about the ferrimagnetic materials is that, they are capable of realizing a considerable fraction of the net magnetization, when removed from the applied magnetic field.

Furthermore, the relation between the flux density B and the applied field intensity H is not linear for these materials. It depends on the previous magnetic history, mechanical and thermal properties as well as on the treatment of the materials being tested. All ferrimagnetic materials have a common property. That is, they have a characteristic temperature i.e. Curie temperature point T_C above which they lose their ferrimagnetic properties and behave as a normal paramagnetic substance.

When a magnetic field H($A.m^{-1}$) is applied to the ferrimagnetic substance, the resulting magnetic flux density B ($wb.m^{-2}$) is composed of the free space and the contribution of the aligned domains. The flux density B can be expressed as follows [18]

$$\mathbf{B} = \mu_o \ (\mathbf{H} + \mathbf{M}) \tag{1-1}$$

Where

$\mu_\circ = 4\pi \times 10^{-7}$ *(wb.m/A)* is the permeability of the free space.

H *($A.m^{-1}$)* is the applied magnetic field intensity.

M *($A.m^{-1)}$* is the intensity of the intrinsic magnetization of the substance.

Equation (1-1) is exact for all substances including ferrimagnetic materials. It is useful to define M by

$$\text{M=} \chi_m \text{H} \tag{1-2}$$

where χ_m is a dimensionless quantity which is known as the magnetic susceptibility of the material.

Substituting equation (1-2) into equation (1-1), this gives

$$B = \mu_o(1 + \chi_m)H$$

$$B = \mu_o\mu_r H = \mu H \qquad (1\text{-}3)$$

Where $\mu_r = 1 + \chi_m$ is a new dimensionless quantity which is known the relative permeability and μ ($\mu = \mu_o\mu_r$) is the permeability of the substance.

1-7-2 Ferrimagnetic Domains

All ferrimagnetic materials consist of many microscopic regions called Wiess domains [19], within them all the magnetic moments are aligned in the same direction. These domains have a volume of about 10^{-12} m^3 to 10^{-8} m^3 and contain 10^{17} to 10^{21} atoms [20]. The magnetizations within the domains are called the intrinsic magnetization per unit mass at temperature T and its value at zero applied magnetic field H is the spontaneous magnetization. The saturation magnetization M_s is the value of the spontaneous magnetization at zero temperature [18].

In unmagnetized sample of the ferrimagnetic substance, the domains are randomly oriented; therefore, the net magnetic moment is zero, as shown in figure (1-4). As shown in figure (1-5-a), the domains are randomly oriented since there is no any an external magnetic field H applied to the unmagnetized sample. When H increases the domains become more aligned in the direction of H by rotating slightly until all of them are nearly aligned as shown in figure (1-5-d). At this state, the saturation condition corresponds to the state where all domains are in the same direction parallel to H, which results in a magnetized sample [19].
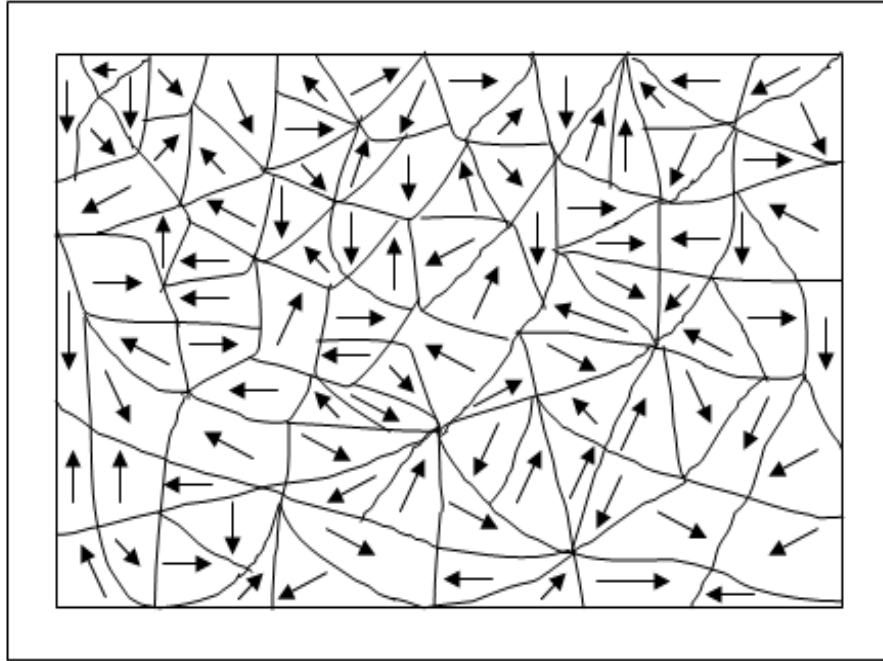
Fig. (1-4): Random orientation spins of an unmagnetized sample of the ferrimagnetic substance.
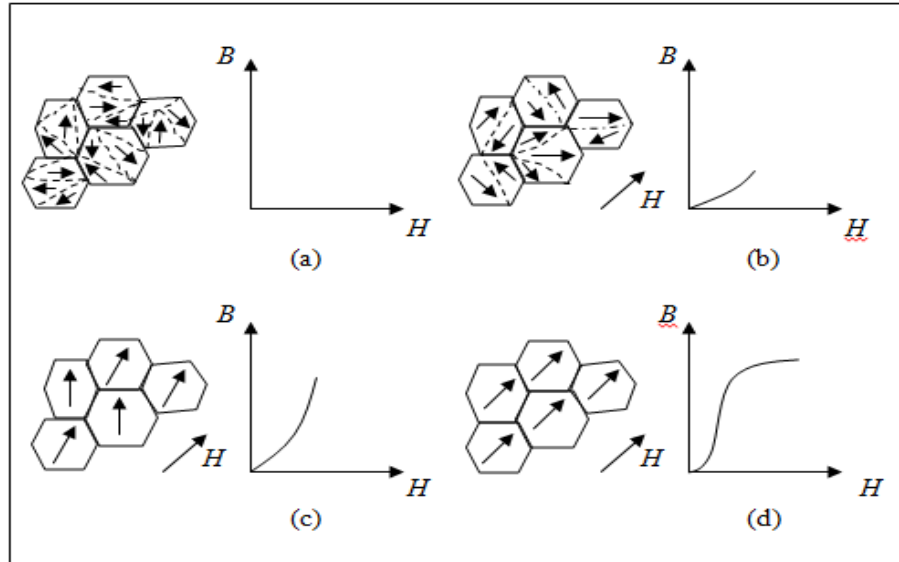
Fig. (1-5): Alignment of Wiess domains.

1-7-3 Magnetic Hysteresis Loop

The relation between B and H for the ferrimagnetic materials was represented by the magnetization curve as illustrated in figure (1-6) [5]. This curve is known as the initial magnetization curve. As shown in the figure (1-6), initially B changes linearly for small values of H. After that, B increases rapidly with increasing of H until it reaches the saturation magnetization state $\mu_o M_s$. Figure(1-6) also shows that as the magnetization reaches the saturation state, the magnetizing field H can be reduced to zero, however, the flux density B follows the original curve, but lags behind the magnetizing field H as illustrated in figure (1-7). This phenomenon just is described called the magnetic hysteresis loop, the word hysteresis literally means to "lag behind", which is a characteristic of all the ferrimagnetic materials. It was shown that the magnetization of these materials depend on the history of the substance as well as the strength of the applied magnetic field.

We can consider that the ferrimagnetic materials have a memory, since; they remain magnetized after the external magnetic field removed [21]. When the magnetizing field **H** reduces to zero, a finite flux density $\pm B_r$ remains, which is known as remanent magnetization, and now the original sample permanently magnetized. In order to reduce the remanent flux density $\pm B_r$ to zero, a negative or a positive magnetization force of magnitude must be applied to the sample. This is defined as the coercivity force $\pm H_C$.

The shape and the size of the magnetic hysteresis loop depend on the properties of the ferrimagnetic materials and the strength of the maximum applied magnetic field.

The enclosed area under the curve of the magnetic hysteresis loop, represents the total work W_H done by the external applied magnetic field per unit volume of the materials through the hysteresis cycle, i.e. during the magnetic process. This work is given by the linear integral [4,17]

$$W_H = \oint_{S'} \mathbf{H}.d\mathbf{B}$$

$$= \frac{1}{\mu_o} [\oint_{S'} \mathbf{H}.d\mathbf{H} + \oint_{S'} \mathbf{H}.d\mathbf{M}_H]$$

$$W_H = \frac{1}{\mu_o} \oint_{S'} \mathbf{H}.d\mathbf{M}_H \qquad \text{(1-4)}$$

Where

S' is the closed area of the magnetic hysteresis loop.

M_H is the component of the magnetization along the direction of the applied magnetic field H.

This integral can be evaluated; since it represents the enclosed area of the magnetic hysteresis loop.

It is now appeared that, the magnetic moments take more energy to produce the magnetization that returned when the magnetization reduced. The energy lost is called the hysteresis loss; it goes into heat.
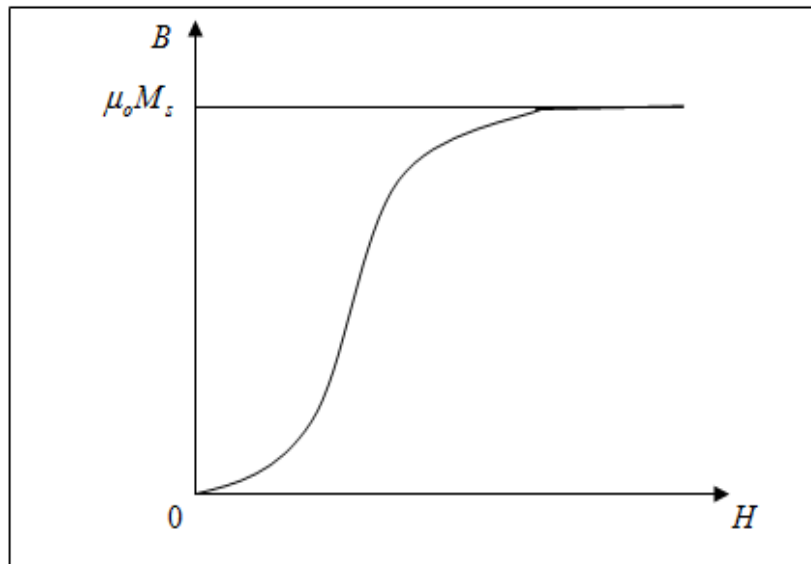
Fig. (1-6): Magnetization curve.
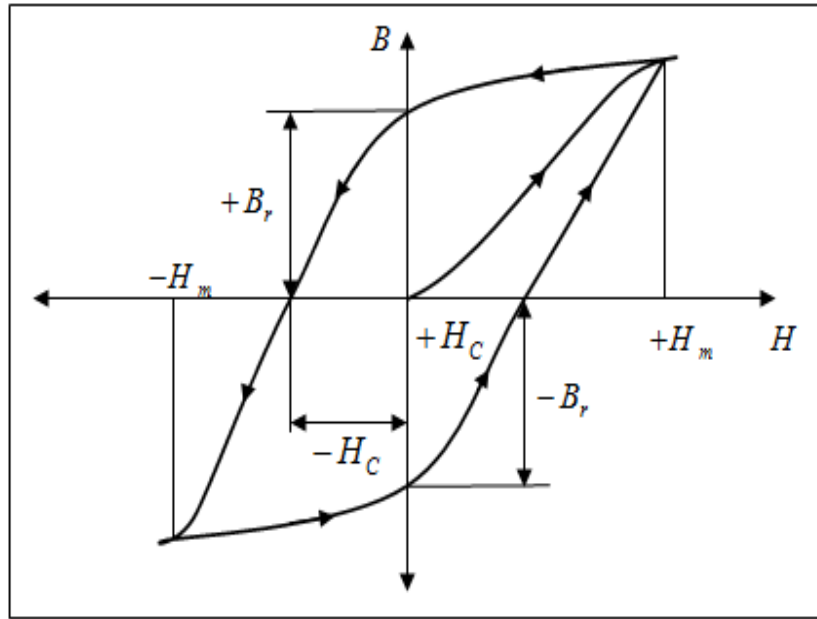
Fig. (1-7): Magnetic hysteresis loop.

1-7-4 Molecular Field Theory of the Ferrimagnetic Materials

In 1948 Neels [22] considered that, a ferrimagnetic crystal lattice could be divided into two magnetic sublattices or groups, i.e. T_d and O_h sites, in the spinel lattice structure, where their magnetic moments are not equal, so that, a net magnetic moment is found. This happens either because they are made from elements in different ionic state, e.g. Fe^{2+} and Fe^{3+}, or from different elements in the same or different ionic states, e.g. Co^{2+} and Fe^{3+} [4]. This can be explained by the molecular field theory of the ferrimagnetic materials.

In order to analyze the ferrimagnetic effects, one needs to calculate the molecular field on each site of a particular atom that caused by an external source and the magnetic atoms in the medium. The molecular magnetization field H_{mT} and H_{mO} of the T_d and the O_h sites, respectively, may be written in the scalar form [5]

$$\begin{pmatrix} H_{mT} \\ H_{mO} \end{pmatrix} = -\begin{pmatrix} N_{TT} & N_{TO} \\ N_{OT} & N_{OO} \end{pmatrix}\begin{pmatrix} M_T \\ M_O \end{pmatrix} \tag{1-5}$$

Where

H_{mT} is the molecular magnetization field acting on the ions at T_d sites.

H_{mO} is the molecular magnetization field acting on the ions at O_h sites.

M_T is the intensity of the intrinsic magnetization within the T_d sites.

M_O is the intensity of the intrinsic magnetization within the O_h sites.

N_{TO} and N_{OT} are the molecular magnetization field constant for the next nearest neighbor interactions between the T_d sites and the O_h sites.

N_{TT} and N_{OO} are the molecular magnetization field constant for the next neighbor interactions within the T_d sites and the O_h sites, respectively.

Here, $N_{TO} > 0$, since the interactions between the two sublattices are antiferromagnetic. The other molecular field constants, N_{TT} and N_{OO}, may in principle be positive or negative, but they are apparent positive for the great majority of the ferrimagnetic materials. They are, also, small compared to N_{TO}, where at equilibrium $N_{TO} = N_{OT}$, however, $N_{TT} \neq N_{OO}$ since the sublattices are crystallographically inequivalent, therefore, $M_T \neq M_O$.

If an external magnetic field H is, also, applied to the ferrimagnetic substance the total magnetic fields H_T and H_O on the atoms at the T_d and the O_h sublattices, respectively, are

$$\begin{pmatrix} H_T \\ H_O \end{pmatrix} = H + \begin{pmatrix} H_{mT} \\ H_{mO} \end{pmatrix} \tag{1-6}$$

Substituting equation (1-5) into equation (1-6), this gives

$$\begin{pmatrix} H_T \\ H_O \end{pmatrix} = H - \begin{pmatrix} N_{TT} & N_{TO} \\ N_{OT} & N_{OO} \end{pmatrix} \begin{pmatrix} M_T \\ M_O \end{pmatrix} \tag{1-7}$$

The magnetization field constants N_{TT} and N_{OO}, can be expressed in terms of N_{TO}. Let $N_{TT} = \alpha N_{TO}$ and $N_{OO} = \beta N_{TO}$ with $N_{TO} = N_{OT}$. This notation is of some

value for temperature region in which the system is ordered [4]. Therefore, equation (1-7) becomes as the following.

$$\begin{pmatrix} H_T \\ H_O \end{pmatrix} = H - \begin{pmatrix} \alpha N_{TO} & N_{TO} \\ N_{OT} & \beta N_{TO} \end{pmatrix} \begin{pmatrix} M_T \\ M_O \end{pmatrix}$$

$$\begin{pmatrix} H_T \\ H_O \end{pmatrix} = H - N_{TO} \begin{pmatrix} \alpha & 1 \\ 1 & \beta \end{pmatrix} \begin{pmatrix} M_T \\ M_O \end{pmatrix} \tag{1-8}$$

Solving for the following matrix

$$\begin{pmatrix} \alpha & 1 \\ 1 & \beta \end{pmatrix} \Rightarrow \begin{cases} = 0 \\ \neq 0 \end{cases} \tag{1-9}$$

According to the equation (1-9), there are two solutions for the above matrix. In the case of zero value the substance may be considered as the antiferromagnetic substance but, in the other case, it may be considered as the ferrimagnetic substance.

The intensity of the intrinsic magnetizations M_T and M_O of each sublattice at thermal equilibrium depends on the spin quantum number S_m for the ions within the sublattices as well as temperature. Therefore, M_T is given by [4]

$$M_T = \sum_i N_i g_i \mu_B S_{mi} B_{S_{mi}}(x_T) \tag{1-10}$$

Where

$$x_T = \frac{S_{mi} g_i \mu_B H_T}{kT} \tag{1-11}$$

and $B_{S_{mi}}(x_T)$ is called **Brillouin** function, which is written in the form [23]

$$B_{S_{mi}}(x_T) = \frac{2S_{mi}+1}{2S_{mi}} \coth(\frac{2S_{mi}+1}{2S_{mi}} x_T) - \frac{1}{2S_{mi}} \coth(\frac{x_T}{2S_{mi}}) \tag{1-12}$$

Likewise, M_O is given by

$$M_O = \sum_j N_j g_j \mu_B S_{mj} B_{S_{mj}}(x_O) \tag{1-13}$$

and

$$x_O = \frac{S_{mj} g_j \mu_B H_O}{kT} \tag{1-14}$$

Where

N_i and N_j are the number of the atoms, i.e. the magnetic ions, per unit volume at the T_d and the O_h sublattices, respectively.

S_{mi} and S_{mj} are the spin quantum number for the atoms at the T_d and the O_h sublattices, respectively.

g_i and g_j are the lande' splitting factor or spectroscopy splitting factor, which is approximately equal to 2.0003 for the free electron.

μ_B is the Bohr magneton and k is the Boltzmann's constant.

The conclusion is that, the magnetization of each sublattice depends on temperature as well as the applied magnetic field. For a very small-applied magnetic field, the spontaneous magnetization of the ferrimagnetic materials changes with increasing of temperature as shown in figure (1-8) [18].

This curve closely follows a mathematical expression known as a Brillouin function. When this decreasing reaches a critical temperature called Curie temperature point T_C or the paramagnetic region, the spontaneous magnetization of the ferrimagnetism vanishes. The temperature dependence of the ferrimagnetic materials below T_C is important. This is because T_C has an effect on the magnetic, the electric and the dielectric properties. It, also, determine the applications of the ferrimagnetic materials.

When the temperature equal T_C , where the applied magnetic field H is constant and very small, therefore, x_T and x_O become very small quantities. The approximation of the Brillouin function may be written by [23]

$$B_{S_m}(x) = \frac{(S_m+1)}{3S_m}x - (\frac{(S_m+1)}{3S_m}\frac{2S_m^2+2S_m+1}{30S_m^2})x^3 \qquad (1\text{-}15)$$

If $x \ll 1$, thus; the second term on the right hand side of the equation (1-15) will decrease to an infinitely small value; so, it will be neglected. Therefore, M_T and M_O are given by [4]

$$M_T = \sum_i N_i g_i \mu_B S_{mi}\left(\frac{S_{mi}+1}{3S_{mi}}\right)x_T \qquad (1\text{-}16)$$

22

and

$$M_O = \sum_j N_j g_j \mu_B S_{mj} \left(\frac{S_{mj} + 1}{3S_{mj}} \right) x_O \tag{1-17}$$

Substituting equation (1-11) into equation (1-16), thus; the M_T is given by

$$M_T = \frac{C_T}{T} H_T \tag{1-18}$$

Similarly substituting equation (1-14) into equation (1-17), thus; the M_O is given by

$$M_O = \frac{C_O}{T} H_O \tag{1-19}$$

with

$$C_{T,O} = \sum_{i,j} N_{i,j} \frac{g_{i,j}^2 \mu_B^2 S_{mi,mj} \left(S_{mi,mj} + 1 \right)}{3k} \tag{1-20}$$

To evaluate the magnetic susceptibility χ_m, that is given by

$$\chi_m = \frac{M}{H} \tag{1-21}$$

where the intensity of the intrinsic magnetization of the magnetic materials may be written in the scalar form M, which is given by [4, 5]

$$M = M_T + M_O \tag{1-22}$$

This implies that

$$\chi_m = \frac{M_T + M_O}{H} \tag{1-23}$$

Upon substituting equation (1-18) and equation (1-19) into equation (1-23), thus; the inverse of χ_m can be written in a more convenient form [4]

$$\frac{1}{\chi_m} = \frac{T}{C} - \frac{1}{\chi_{mo}} - \frac{\delta}{T - \theta'} \tag{1-24}$$

where C is the **Curie** constant which is given by $C = C_T + C_O$, and

$$\frac{1}{\chi_{mo}} = -\frac{1}{C}(C_T^2 N_{TT} + C_O^2 N_{OO} + 2C_T C_O N_{TO})$$

$$\delta = -\frac{C_T C_O}{C^3}\{C_T^2(N_{TT} - N_{TO})^2 + C_O^2(N_{OO} - N_{TO})^2$$

$$-2C_T C_O[N_{TO}^2 - (N_{TT} + N_{OO})N_{TO} + N_{TT}N_{OO}]\}$$

$$\theta' = -\frac{C_T C_O}{C}(N_{TT} + N_{OO} - 2N_{TO})$$

Ferrimagnetic materials become paramagnetic above Curie temperature point and in this region the graphical representation of the equation (1-24) is a hyperbola as shown in figure (1-9). In the limit at large temperature, i.e. $T \rightarrow \infty$, the last term in equation (1-24) disappears, but the asymptote equation (1-24) is given by the remains terms

$$\frac{1}{\chi_m} = \frac{T}{C} - \frac{1}{\chi_{mo}} \tag{1-25}$$

If γ is defined as the T-intercept found by extrapolation of the line, then, $\gamma = -C/\chi_{mo}$, Neel's called this asymptotic Curie temperature point. Therefore, the equation (1-25) becomes

$$\chi_m = \frac{C}{T + \gamma} \tag{1-26}$$

This means that, when temperature is equal to **Curie** temperature point the ferrimagnetic substance will be considered as the paramagnetic substance, which does not obey to the Curie-Wiess law
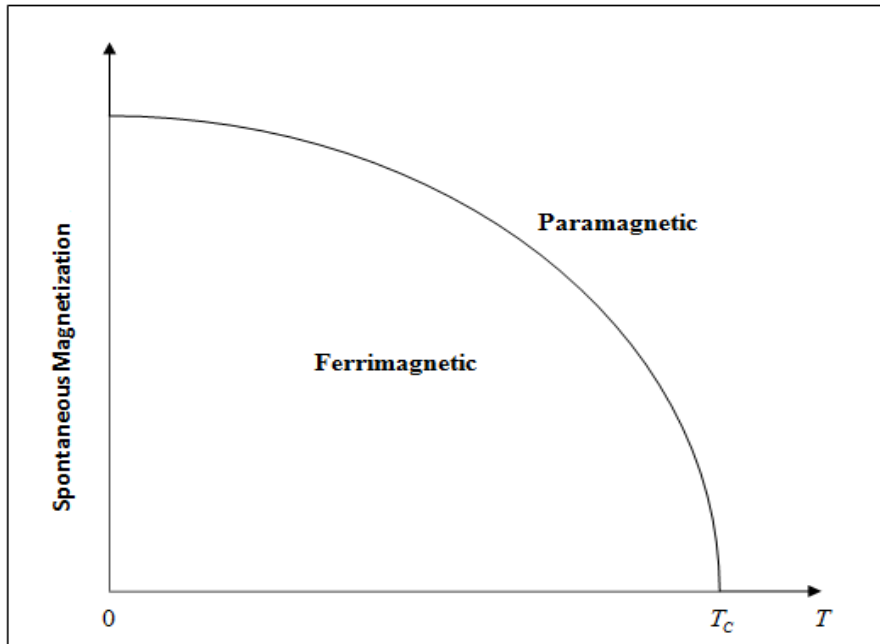
**Fig. (1-8): Spontaneous magnetization of the ferrimagnetic
materials as a function of the absolute temperature**
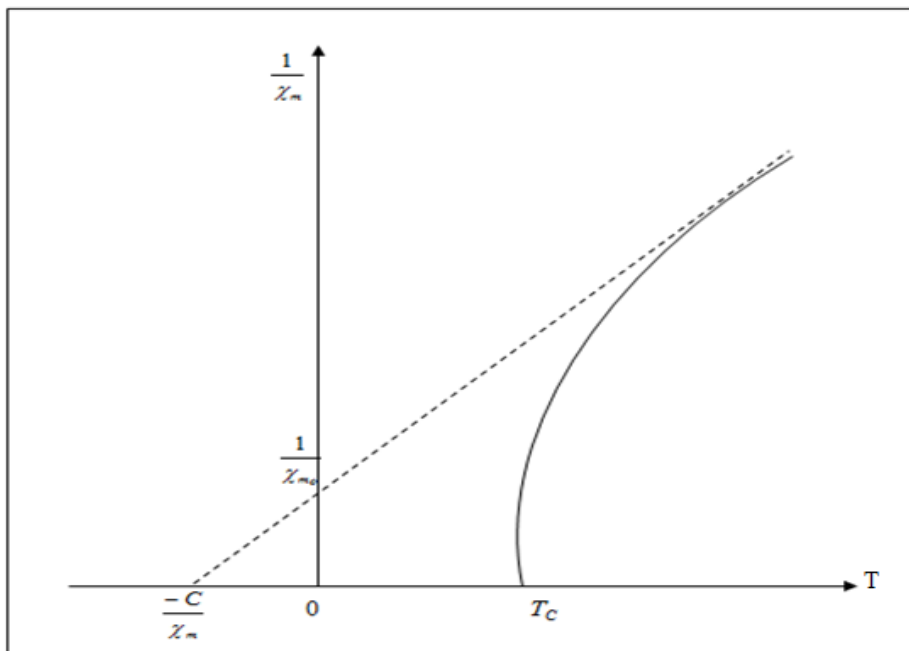
**Fig. (1-9): Inverse magnetic susceptibility of the ferrimagnetic materials above the T_C
according to the molecular field theory.**

1-8 Electric Properties of the Ferrimagnetic Materials

Ferrimagnetic materials are of greater commercial application in the electromagnetic interfaces known as EMI, which is used in hard disk drives, in laptops and other electronic products. Generally, the electrical conductivity of ferrites increases with the increase of temperature, which shows that ferrites have semiconductor behavior. Ferrites have very high resistivity which is one of the considerations for microwave applications ,The electrical properties of ferrites are sensitive to preparation method, sintering temperature, sintering time, rate of heating and rate of cooling [24,25]. The study of electrical conductivity produces valuable information on behavior of free and localized electric charge carried in the sample.

1-8-1 conductivity of the Ferrimagnetic Materials

The conductivity σ of the ferrimagnetic materials depends on temperature and the measuring frequency of the applied field. This is controlled by the cations concentration on the sites of the spinel lattice structure [26]. Therefore, their conductivity can be expressed according to [2]

$$\sigma = \sigma_o e^{-E_a/kT}$$ (1-27)

where $\sigma_\circ$ is the temperature dependent constant, E_a represents the activation energy, which is the energy required to release an electron from the ion for a jump to the neighboring ion, so that, giving rise the electric conductivity, and K is Boltzmann constant .

Almost all of the known ferrimagnetic materials are poor conductors of electricity. In the early days, the ferrimagnetic materials with high resistivity are called ferrites. Therefore, the resistivity ρ of the ferrites at room temperature varies from $10^{-2}\Omega.cm$ to $10^{11}\Omega.cm$, which depends on the chemical composition [6].

1-8-2 Conduction Mechanism in the Ferrimagnetic Materials

The conduction mechanism in the ferrimagnetic materials is different and much less understood in comparison with the elements in-group IV semiconductors such silicon and germanium [26].

In the ferrimagnetic materials, the concentration of the charge carriers is larger than semiconductor materials [14]. The nature of charge carriers in ferrimagnetic oxides have been the subject of many experimental and theoretical studies, however, until now no conclusive theory has been formulated for the conduction mechanism in these materials [28].

The conduction mechanism is attributed to the hopping of the electrons between Fe^{2+} ions and Fe^{3+} ions. The Fe^{2+} ions are considered the donors that contain extra electron, which will jump to the adjacent Fe^{3+} ions easily and will constitute the electrons conduction. The oxidation of the divalent iron ions reduces donor content in the material such that, the electric resistivity is increased [29].

The conductivity in the ferrites associates with the presence of the ions for the element in more than one valence state; these ions are distributed over the crystallographically inequivalent sites [26]. The conduction mechanism of the ferrites depends on temperature. Therefore, the conductivity will be described as in equation (1-27).

The detailed behavior of the complex compounds such that ferrimagnetic materials are not well understood. In general, The conduction at lower temperature is due to hopping electron between $Fe^{2+} \Leftrightarrow Fe^{3+}$ ions [30], whereas at a higher temperature is due to the hopping polarons [31, 32].

Since the mobile carriers have spin magnetic moments, they are strongly influenced in their motion by the direction of spins on neighboring sites. And they can polarize the lattice sites. Therefore, the combination of the mobile carriers and lattice polarization is known as a magnetic polaron [17]. It is found that, the neighboring spins forming a"magnetic polaron". However, the motion of the polaron is always characterized by a large effective massed and low mobility. If the polarization is much localized the polaron is called small polaron and usually moves

bythermal activation. At high temperatures, the electron moves from site to site by thermally activated hopping; at low temperature the electron tunnels slowly through the crystal [15]. In the neighborhood of T_C thermal vibrations are disordering spins. The motion of a charge carrier may be strongly influenced by the scattering produced by the disordered spins.

1-9 Dielectric Properties of the Ferrimagnetic Materials

The polycrystalline ferrites, which have many applications at microwave frequencies are very good dielectric materials. The dielectric properties of the ferrites depend on several factors including [33] the method of preparation, Sintering temperature, Sintering atmosphere, Frequency applied and chemical composition.

When a ferrite powder is sintered under gradually reducing conduction the divalent iron ions are formed in the bulk. This leads to high conductivity ferrite grains, which has a very high dielectric constant ε [34]. The electrons exchange interaction between the Fe^{2+} ions and the Fe^{3+} ions result in a local displacement of the electrons in the direction of the electric field. This determines the polarization of the ferrites. Therefore, the Fe^{2+} ions play a dominant role in the mechanisms of the conductivity and the electric polarization. The concentration of the Fe^{2+} ions depends on sintering temperature and sintering atmosphere [35].

1-9-1 Dielectric Theory of the Ferrimagnetic Materials

Measurements by **Blechstein** [36] showed that, the of manganese ferrite have an astonishingly high apparent dielectric constant. Brockman [37] found such high dielectric constant in ferrimagnetic cores made of ferrites that had been developed at laboratory [38]. In order to obtain more quantitative information about the behavior of the ferrite, impedance measurements were carried out with disks of several compositios.

In general, the dielectric constant is roughly inversely proportional to the square root of the resistivity. Both quantities depend on the measuring frequency of the applied field [6].

Maxwell-Wagner two layer model was used to explain the high apparent permittivity at low frequency dispersion in polycrystalline ferrites [39,40], A well-conducting bulk material with conductivity σ_1, permittivity ε_1 and thickness d_1 is separated by poorly conducting layers with conductivity σ_2, permittivity ε_2 and thickness d_2. From the equivalent layer model of figure (1-10), the permittivity ε and the effective conductivity σ can be obtained as a function of the frequency. The dispersion formula for the permittivity ε and the conductivity σ can be described by the terms in the form [5, 6]

$$\sigma = \sigma_{hv} + \frac{\sigma_{lv} - \sigma_{hv}}{1+(\omega\tau_\sigma)^2} \tag{1-28}$$

$$\varepsilon = \varepsilon_{hv} + \frac{\varepsilon_{lv} - \varepsilon_{hv}}{1+(\omega\tau_\varepsilon)^2} \tag{1-29}$$

Where, the indices lv and hv indicate the limiting values at low and high frequency, respectively. The relaxation time τ is a characteristic time constant of ferrites. Thus; the relaxation frequency $\omega \propto 1/\tau$ for the different materials appears to be approximate proportional to the low-frequency value of the dielectric constant [6].

Referring to the figure (1-10), suppose that z is defined by the ratio between the thickness of the grains boundary layer (d_2) and the thickness of the ferrite grains layer (d_1), which is written by

$$z = \frac{d_2}{d_1} \tag{1-30}$$

Suppose that $z \ll 1$, then the parameters σ_{hv}, σ_{lv} and τ_σ in the equation (1-28) can be given as the follows [39]

$$\sigma_{hv} = \frac{\sigma_1\sigma_2(\varepsilon_1 + z\varepsilon_2)^2}{\sigma_1\varepsilon_1^2 + z\sigma_2\varepsilon_2^2} \tag{1-31}$$

$$\sigma_{lv} = z\sigma_1 + \sigma_2 \tag{1-32}$$

$$\tau_\sigma = \varepsilon_o \left(\frac{\sigma_1\sigma_2(\sigma_1\varepsilon_1^2 + z\sigma_2\varepsilon_2^2)}{z\sigma_1 + \sigma_2} \right)^{\frac{1}{2}} \tag{1-33}$$

In the same way, the parameters ε_{hv}, ε_{lv} and τ_ε in the equation (1-29) can be given as the follows

$$\varepsilon_{hv} = \frac{\varepsilon_1 \varepsilon_2}{\varepsilon_1 + z\varepsilon_2} \tag{1-34}$$

$$\varepsilon_{lv} = \frac{\sigma_2^2 \varepsilon_2 + z\sigma_1^2 \varepsilon_1}{(z\sigma_1 + \sigma_2)^2} \tag{1-35}$$

$$\tau_\varepsilon = \varepsilon_o \left(\frac{\sigma_1 \sigma_2 (\varepsilon_1 + z\varepsilon_2)}{z\sigma_1 + \sigma_2} \right) \tag{1-36}$$

It can be found that, the relation between τ_ε and τ_σ is given by [39]

$$\tau_\varepsilon = \left(\frac{\sigma_{hv}}{\sigma_{lv}} \right)^{1/2} \tau_\sigma \tag{1-37}$$

This phenomenological theory is generally used to describe the dielectric relaxation in the ferrites at constant temperature mostly room temperature. The idea of this investigation was to find out whether the inhomogeneity model holds for the variation of temperature
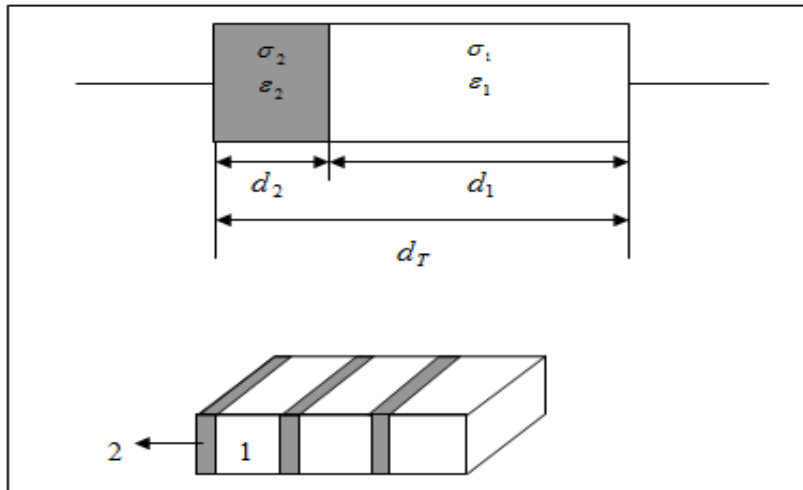
Fig. (1-10): Equivalent layers model of the Maxwell-Wagner theory.

1-9-2 Dielectric Loss Tangent

A study of the dielectric properties of the ferrimagnetic materials is interesting and has practical value. When an *AC* voltage is applied to a circuit containing a capacitor, only the displacement current I_D or the capacitive current I_C will flow across the capacitor if the material filling the capacitor is a perfect dielectric. In that case no electromagnetic energy will be lost in the capacitor. Since perfect dielectrics hardly exist, there is usually a resistive current, $I_{Res.} = V_{in}/R_{in}$ running through the material, as well as the displacement current. The resistive current is responsible for the energy losses in the dielectric materials. The resistive component of the total current is in phase with the voltage applied to the capacitor [41].

Let the applied voltage due to the capacitor V_C in an *AC* voltage circuit containing a capacitor is given by

$$V_C = V_T e^{i\omega t} \tag{1-38}$$

then, the charge Q on the capacitor of the capacitance C_a is

$$Q = C_a V_T e^{i\omega t} = \varepsilon C_o V_T e^{i\omega t} \tag{1-39}$$

where

       C_o is the value of the capacitance of the vacuum.

       ε is the dielectric permittivity or dielectric constant of the material.

The capacitive current I_C is defined by

$$I_C = \frac{dQ}{dt} = i\omega\varepsilon C_o V_C \tag{1-40}$$

To account for the energy losses a complex dielectric constant is thus; introduced

$$\varepsilon = \varepsilon' - i\varepsilon'' \tag{1-41}$$

where

       ε' is the dielectric constant or true permittivity dielectric constant which described expressed to the stored energy in the material.

       ε'' is the dielectric loss factor or the imaginary permittivity dielectric loss and it described the dissipative energy in the material which is given by [42]

$$\varepsilon'' = 2\pi\varepsilon_o \frac{\sigma_a}{\nu} = \frac{\sigma_a}{\nu} 1.8 \text{X} 10^{10} \qquad (1\text{-}42)$$

with ε_o is the permittivity of the free space $(10^{-9}/36\pi) F.m^{-1}$ and σ_a is the active volume conductivity. Its magnitude is given by the following relation [42]

$$\sigma_a = \nu \frac{\varepsilon \tan \delta}{1.8 \text{X} 10^{10}} \Omega^{-1} m^{-1} \qquad (1\text{-}43)$$

where ν is the frequency of the applied field and $\tan(\delta)$ is the dielectric loss tangent, which is a component of the phase difference between the applied voltage and the total current through the circuit .

The dielectric loss tangent D is given by [42]

$$D = \tan\delta = \frac{\varepsilon''}{\varepsilon'} \qquad (1\text{-}44)$$

The quantity $\tan(\delta)$ sometimes called dissipation factor. As well as the other parameters of the dielectric properties, the value of $\tan(\delta)$ depend on the various external factors such as frequency of the applied voltage.

The behavior of $\tan(\delta)$ with an applied frequency is represented in figure (1-11). The frequency ω' corresponds to the maximum $\tan(\delta_{max})$ as illustrated in figure (1-11). It is given by [41]

$$\omega' = \sqrt{\frac{1}{\tau^2} + \frac{S_C}{C_g \tau}} \qquad (1\text{-}45)$$

with

$$\tan(\delta_{max}) = \frac{S_C \tau}{2C_g \sqrt{1 + (S_C \tau / C_g)}} \qquad (1\text{-}46)$$

where

      C_g is the geometrical capacitance.

      S_C is the conduction corresponding to absorption current I_A.

Figure (1-11) becomes especial clear from a physical standpoint in the case of a purely dipole mechanism of losses: the frequency ω' corresponds to such a ratio between the period of an external electric field and the time τ of the relaxation of

the dipoles, as it is needed to observe the greatest loss of energy to overcome the resistance of the viscous medium by the dipole. Assuming that $S_C \ll C_g \tau$, then equation (1-45) becomes

$$\omega'\tau = 1 \qquad\qquad (1\text{-}47)$$

with $\omega' = 2\pi v_{max}$ which is defined as the jumping probability per unit time, i.e. hopping probability P, where τ is the relaxation time which is given by the relation ($\tau = 1/2P$ or $v_{max.} \propto P$) [43,44].

Equation (1-47) is the condition of the maximum of dielectric losses in the polar dielectric materials.
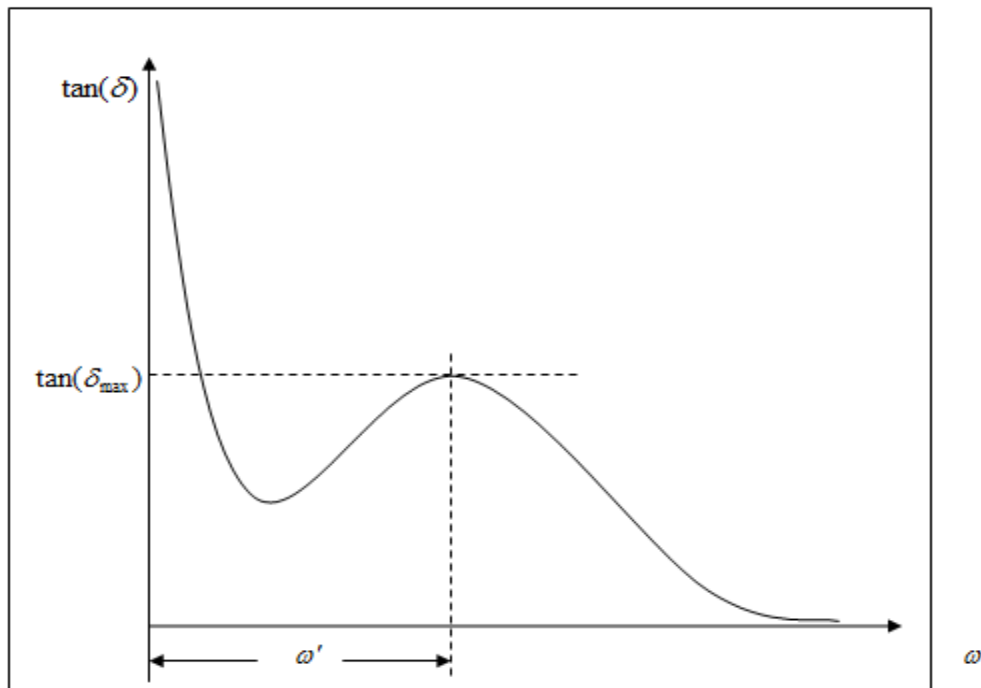
**Fig. (1-11): Dependence of the loss tangent of the dielectric
materials on the applied frequency**

CHAPTER II

LITERATURE SURVEY

2-1 Introduction

This chapter contains some of the previous studies for various ferrite systems which have the same trend of the subject of the mixed *Ni-Zn* spinel ferrite. Some of these studies have used *IR* spectra to illustrate the structure of spinel lattice. Other studies have illustrated the magnetic, the electric and the dielectric properties for different ferrite systems.

2-2 Structure of the Spinel Lattice

Binu P.Jacob et al,[45] , studied the *FTIR* spectra for the ferrite systems of $NiTb_xFe_{2-x}O_4$, which have been prepared using sol-gel technique . Two main absorption bands are seen in the infrared spectra of spinel ferrites. The higher band ν_1 observed in the range 600-550 cm^{-1} , The lowest band ν_2 observed in the range 450-385 cm^{-1} .

Mazen [46] , studied IR spectra of Zn^{2+} ions substituted Li-Mg ferrites that having formula $Li_xMg_{0.4}Zn_{0.6\ -x}Fe_{2+x}O_4$. All samples show two prominent absorption bands , higher bands ν_1 found to lie in the range (615- 565)cm^{-1} and lower bands ν_2 in the range (430-420) cm^{-1} as the concentration of Zn^{2+} ions increases. They also found that the center frequency of the principle bands ν_1 and ν_2 shift gradually toward the low frequency with addition Zn^{2+}ions .

El-Sayed, [47], studied the IR spectra of ferrite samples of $Ni_{1-x}Zn_xFe_2O_4$ system at room temperature from (200-1300) cm^{-1} .The IR spectra have shown three main absorption bands below (1000) cm^{-1} , ν_1 =570 cm^{-1} , ν_2 =400 cm^{-1} and ν_3 = 240 cm^{-1} .He found that the bands ν_2 and ν_3 increase by Zn^{2+} ions .

2-3 Magnetic Properties

Upadhyay et al, [48], studied the magnetic properties for the mixed ferrite system of $Mn_{1-x}Zn_xFe_2O_4$. They reported that, the Zn^{2+} ions have a strong preference at the T_d sites, while the Mn^{2+} ions occupied the O_h sites and the Zn spinel ferrite spectrum result in only super-paramagnetic spectrum only.

Jadhav, [49], studied the magnetic properties for the Zn^{2+} ions substituted on the mixed Li-Cu ferrite in the form $Li_xCu_{0.4}Zn_{0.6-2x}Fe_{2+x}O_4$. He showed that, the magnetization increased with increasing of the Zn^{2+} ions until it reached the maximum value for $x = 0.3$, then it decreased by adding the Zn^{2+} ions. They noticed that, the initial permeability increased slowly with increasing of temperature till reached a maximum value and then it sharply dropped to zero at **Curie** temperature point, which decreased continuously with increasing of the Zn^{2+} ions.

2-4 Electric Properties

Davinder et al, [50], studied the electric conductivity of polycrystalline $Mn_{1-x}Zn_xFe_2O_4$ ferrites . They showed that the value of the electric conductivity increases with increased of Zn^{2+} ions . The plot of log (σ T) versus (10^3/T) were increase with increasing of temperature and it showed transition near Curie temperature point.

U. Ghazanfar et al, [51], studied the electric properties for the mixed *Ni-Zn* ferrite system in the form $Ni_xZn_{1-x}Fe_2O_4$. They found that at room temperature DC resistivity increases by increasing Ni, and they found that the samples having higher values of resistivity also have higher values of activation energies and vice versa.

El–Shabasy, [52], studied DC electrical resistivity was for $Zn_xNi_{1-x}Fe_2O_4$ samples (with x = 0, 0.2, 0.4, 0.6, 0.8 and 1) prepared using the usual ceramic technique as function of temperature T and composition x. The DC electrical resistivity ρ, and activation energies for electric conduction in ferrimagnetic (E_f) and in paramagnetic (Ep) region decrease as zinc ion substitution increases. The ferrite samples studied have a semiconductor behavior where electrical resistivity ρ decreases on increasing the temperature. The activation energy for the electric conduction in the paramagnetic region was found to be higher than that in the ferrimagnetic region.

2-5 Dielectric Properties

RaviKumar et al, [53], studied the dielectric constant ε and dielectric loss tangent $\tan(\delta)$ for the polycrystalline mixed *Mn-Zn-Gd* ferrite in the form $Mn_{0.58}Zn_{0.37}Fe_{2.05-x}Er_xO_4$. The values of ε and $\tan(\delta)$ were measured at room temperature in the applied frequency range (1-13)*MHz*. They observed that the variation of ε and $\tan(\delta)$ with the applied frequency showed a normal dielectric behavior of spinel ferrite.

P.A. Jadhav et al, [54], prepared fine powders of Ni-Cu-Zn ferrite with composition $Ni_{(0.7-x)}Cu_xZn_{0.3}Fe_2O_4$ (where x=0, 0.2, 0.4 and 0.6) by the citrate precursor method and measured Dielectric constant (έ) and loss tangent (tan δ) as a function of frequency. The έ and tan δ showed a decreasing trend with increase of frequency for all their samples.

J. Azadmanjiri [55], studied the dielectric properties for the mixed *Ni-Zn* ferrite system in the form $Ni_{1-x}Zn_xFe_2O_4$,which were prepared by the chemical sol-gel method ,where x=(0,0.1,0.2,0.3,0.4). He found that Zn content has a significant influence on the electromagnetic properties such as dielectric constant (ε)and dielectric loss tangent (tanδ) , these values decrease with increasing of zinc.

CHAPTER III

EXPERIMENTAL TECHNIQUES AND APPARATUS

3-1 Introduction

This chapter explains the experimental techniques which includes a description of the preparation method of the ferrite samples "The Oxide Method". The Fourier transform infrared analysis FT-IR spectra were recorded in order to confirm the formation of spinel ferrite, the method of measuring the induction as a function of temperature and the magnetization as a function of a magnetizing field is described. Also, *DC* conductivity and the dielectric properties are determined. In addition, the apparatus and the electric circuits that used are illustrated throughout this chapter.

3-2 Preparation of Samples "The Oxide Method".

Polycrystalline ferrites are usually formed by some types of solid state reaction . The mixed ferrites $Ni_{1-x}Zn_xFe_2O_4$, where x is the percentage increment of Zn^{2+} ions on the compound which have the value $x= 0.0, 0.2 , 0.4 , 0.6 , 0.8$ and 1.0 , were prepared by using the standard double sintering ceramic technique by mixing pure metal oxides in the calculated proportions according to the equation

$$(1- x) \text{ NiO} + x \text{ ZnO} + \text{ Fe}_2\text{O}_3 \longrightarrow \text{Ni}_{1-x} \text{Zn}_x\text{Fe}_2\text{O}_4$$
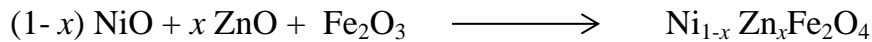
High purity oxide materials have been used for the preparation of the investigated polycrystalline ferrites. The weight of each oxide was calculated and listed in table (3-1)

Table (3-1): Weight of each oxide used to prepare the various samples of the mixed *Ni-Zn* spinel ferrite.

x	The Result composition	M.Wt. of *NiO* in (gm)	M.Wt. of *ZnO in (gm)*	M.Wt. of *Fe₂O₃* in (gm)
0.0	Ni Fe$_2$ O$_4$	7.9666	0.0	17.0333
0.2	Zn$_{0.2}$ Ni$_{0.8}$ Fe$_2$ O$_4$	6.3370	1.7263	16.9365
0.4	Zn$_{0.4}$ Ni$_{0.6}$ Fe$_2$ O$_4$	4.7259	3.4332	16.8407
0.6	Zn$_{0.6}$ Ni$_{0.4}$ Fe$_2$ O$_4$	3.1329	5.1209	16.7461
0.8	Zn$_{0.8}$ Ni$_{0.2}$ Fe$_2$ O$_4$	1.5576	6.7897	16.6525
1.0	Zn Fe$_2$ O$_4$	0.0	8.4400	16.5599

Twenty five grams from the oxide materials were used for the preparation of each composition. The materials were weighted using a sensitive electric balance (ADAM model PW124) with an accuracy 1×10^{-4} gm.

The weighted materials were mixed and then grounded to a very fine powder for 5 hours. The mixed powder of oxides was presintered at 750 C° for 3 hours soaking time using a laboratory Furances (BIFATHERM model AC62).

Then the prefired powder was well ground for 3 hours and pressed with hydraulic press under constant pressure of 3×10^{8} pa, by using a small quantity of butyl alcohol as a binding material. Some samples were pressed in the form of a disc shape which have a diameter 11 mm and thickness L (5 - 6.3) mm. Other samples in the form of toroids with an external diameter r_o of 9.3mm, and internal diameter r_i of 4.7mm with thickness of (4-5) mm.

All samples were sintered at $1200^{o}C$ for soaking time of 5 hours using a laboratory Furances (BIFATHERM model A C62). After sintering, the samples were cooled down gradually to room temperature. After cooling, the discs samples were polished to obtain the form of circular discs having two uniform parallel surfaces, and it used to measure the DC electrical conductivity, the dielectric constant and dielectric loss tangent. The toroidal samples were polished to obtain a uniform shape to measure the magnetization properties.

3-3 FT-IR Spectroscopy Measurements

For recording the FT- IR spectra, the powder of the samples was mixed with Potasium Bromide KBr at a ratio of 1:200 by weight to uniform dispersion in KBr pellet. The mixed powder of samples were pressed at 3×10^{8} pa by a hydraulic press. Clean discs with a thickness approximate of   1.0mm were obtained . FT-IR spectra in the range from 350 cm^{-1} to $1000cm^{-1}$ were recorded at room temperature using FT-IR Spectrophotometer (Cary 660 FT-IR spectrometer) .

3-4 Measurements of the Magnetic Properties

The measurement of the magnetization M was based on Faraday's law of the electromagnetic induction, using the toroidal sample as shown in figure (3-1). The toroidal samples of the ferrites materials are especially used as a transformer core in the magnetization measurements. Different parameters can be defined from the figure (3-1) as:

L   is the toroidal sample thickness. It was measured by a micrometer with accuracy $0.01mm$.

r_i is the internal radius of the toroidal sample.

r_o is the external radius of the toroidal sample.

r_m is the average radius of the internal and the external radius of the toroidal sample i.e. $r_m = \dfrac{r_i + r_o}{2}$
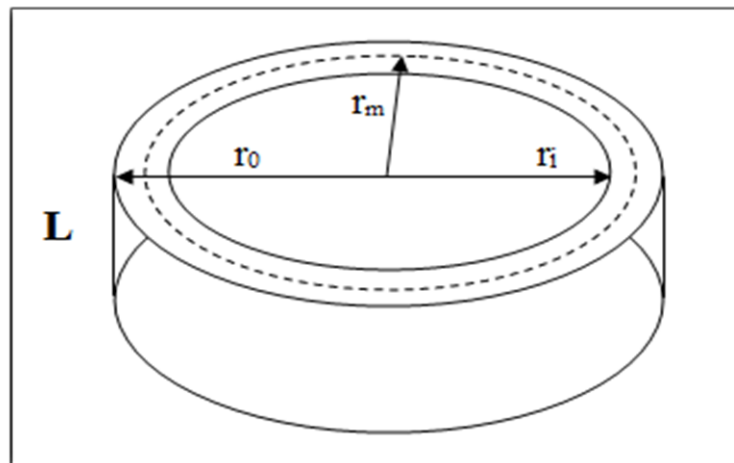

Fig. (3-1): A toroidal sample shape.

3-4-1 Magnetization Measurements

The magnetization M (Am^{-1}) was measured at room temperature as a function of the applied magnetizing current which changed in the range from (0 -5A) at constant magnetizing frequency ν = 50Hz. The corresponding applied magnetic field H (Am^{-1}) varied in the range of (0-3500 Am^{-1}). Which was calculated by the equation (3-3). The used circuit in these measurements is shown in figure (3-2).

The magnetization M (Am^{-1}) was calculated from the relation

$$M = \frac{B}{\mu_o} - H \tag{3-1}$$

The scalar quantity of the flux density B was calculated according to [54]

$$B = \frac{50}{\nu} \frac{50}{AN_S} V_S \tag{3-2}$$

Where:

   V_s is the induced voltage in the secondary coil,

   N_s is the number of turns of secondary coil,

   A is the cross sectional area of the toroidal sample [A=L(r_o-r_i)]

   H is the applied magnetic field which calculated from the relation [5]

$$H = \frac{N_P i_P}{2\pi r_m} \tag{3-3}$$

Where:

   N_p is the number of turns of primary coil

   i_p is the current in the primary coil

   r_m is the average radius of the internal and the external radius of the toroidal

   sample i.e. $r_m = \frac{r_i + r_o}{2}$
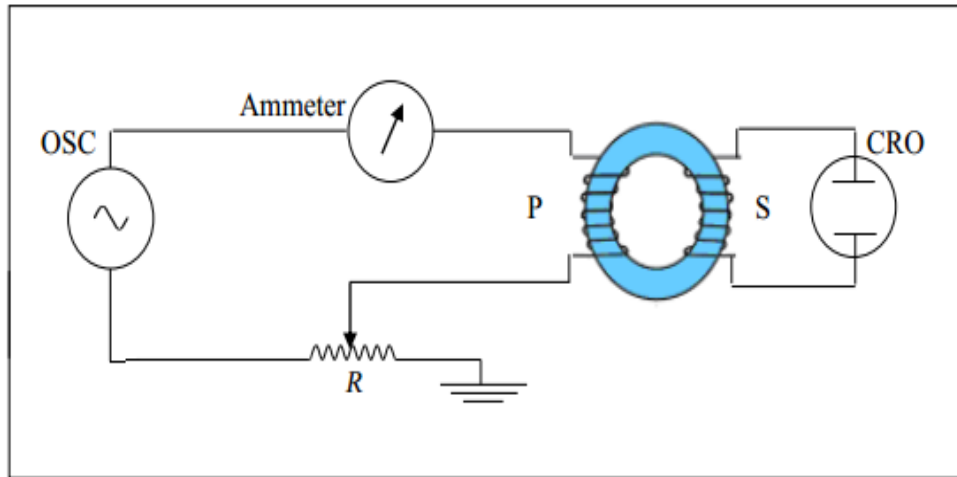
Fig. (3-2): Circuit diagram for measuring the magnetization using the toroidal samples of the mixed *Ni –Zn* spinel ferrite.

3-5 Temperature Measurements

For the purpose of temperaturre measurement ,at the sample in the case of all measurement, a thermocouple of type K(NiCr–NiAI) was used to measure temperature from room temperature up to 773k . A digital multimeter temperature indicator (model 2010DMM) with resolution 1K was connected with the thermocouple.

3-6 Measurements of inductance

To determine the curie point temperature, the inductance L of the toroid as a function of temperature was measured, the inductance L was measured directly by LCR meter model (GW- instek LCR-821) , with series circuit and applied voltage of 1v and constant frequency of 20 KHz with accuracy of (0.05%) .

An insulated coil that is a wire woned on a ring –shaped "toroid" which made of ferrite samples , the numbers of turns was 14 turns.
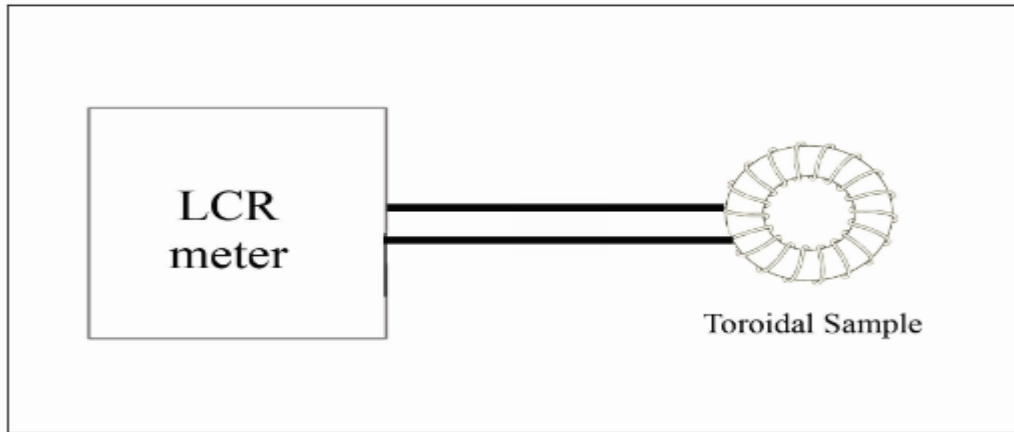
Fig (3-3) Circuit diagram for measuring the inductance using the toroidal samples of the mixed *Ni –Zn* spinel ferrite.

3-7 Measurement of Electrical Properties

In DC electrical conductivity Properties ,the current was measured at different temperature using the two-probe method . Pellets of a disk-shape were polished and smoothed to have uniform plane surface. Silver was pasted on both sides to ensure good electrical contacts. Two silver wires with high purity were used as electrodes.

3-7-1 Measurements of DC Electrical Conductivity

A digital multimeter (model FLUKE -177) was used to measure the resistance of the samples.

The specific *DC* electric conductivity (σ_{DC}) $\Omega^{-1}m^{-1}$ of the samples were calculated from the formula :

$$\sigma_{DC} = R^{-1}\frac{L}{A} \qquad (3\text{-}4)$$

Where:-

   R: Resistance of the sample

   L : Length of the sample which was measured by a micrometer of accuracy 0.01 *mm*

   A: Cross –sectional area of the sample .

The electrical conductivity was measured in wide range of temperature, from room temperature up to 773K with three-degrees step. The increasing of temperature was carried out gradually.

3-8 Measurement of the Dielectric Properties

To   measure dielectric constant and dielectric loss tangent over a variable range frequency in range of 10^4 to 10^6 Hz at room temperature . An **AC** field was established across the sample as indicated in fig (3 -3) , which consists of:

1- Function   signal generator power amplifier (OSC)(model MFG-8250A) was connected across the sample S and standard non inductive resistance R, where the value of   R depends upon the resistance of the each sample.

2- Adual-channel oscilloscope (CRO) (GW modelGOS-620) used to measure:

i- The total input voltage V_T connect on X- channel .

ii-The potential V_R drop across the standard non inductive resistance connect on Y- channel .

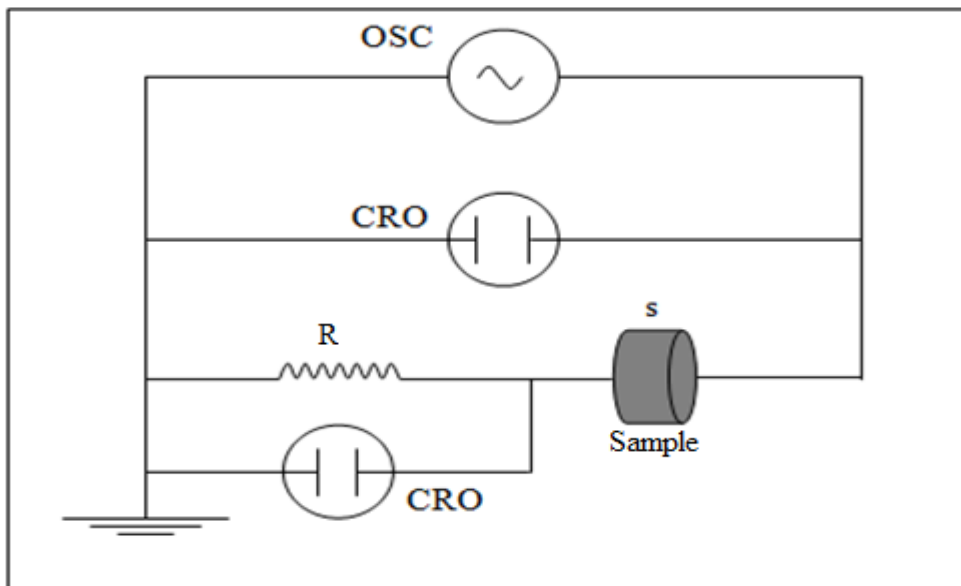**Fig. (3-4): Circuit diagram for measuring the dielectric loss tangent using the disc samples of the mixed Ni-Zn spinel ferrite.**

Since AC current passing through the sample have the same of the AC current passing through the resistance R . It can be calculated from Ohm's Law $I_T = V_R / R$.

According to Collett et al [56] , values of loss tangent were obtained from Lissajous figure displayed on along persistence cathode ray oscilloscope . Referring to figure (3-4), let V_T be the voltage applied to X- plates and V_R to Y plates .

If $$V_X = V_T \sin(\omega t) \qquad (3-6)$$

Then $$V_Y = V_R \sin(\omega t - \varphi) \qquad (3-7)$$

Where φ is the phase angle. These two signals form a Lissajous figure as shown in the figure (3-5). Referring to this figure, when $V_Y = 0$, then $V_X = V_\theta$

If $V_Y = 0$, this implies that $(\omega t + \phi) = \pi$ or $\omega t = \pi - \phi$.

Therefore, we find that

$$V_\theta = V_T \sin(\pi - \varphi)$$

$$V_\theta = V_T \sin(\varphi) \qquad (3-8)$$

Hence, the dielectric loss tangent D was given by the following:

$$D = \tan \delta = \cot \varphi \qquad (3-9)$$

$$D = = \frac{\sqrt{(V_T^2 - V_\theta^2)}}{V_\theta} \qquad (3-10)$$

where V_T and V_θ can be readily measured on the cathode ray oscilloscope, then the value of D at a given frequency can be computed from the equation (3-10) [57].
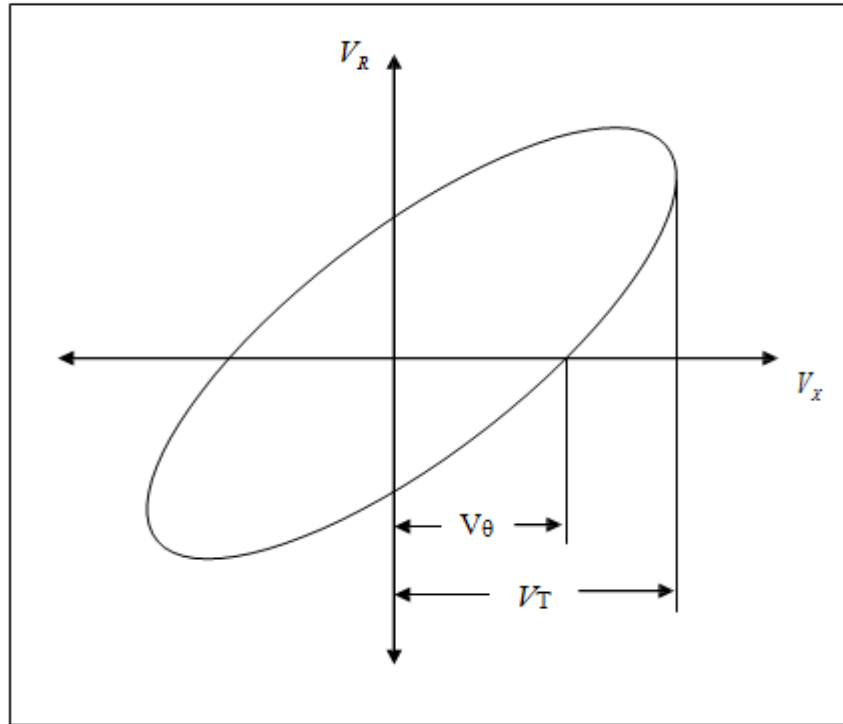
Fig. (3-5): Lissajous figure of the input voltage V_T and the current passing through the sample.

CHAPTER IV

RESULTS AND DISCUSSION

4-1 Introduction

This chapter includes the obtained results and the discussion of the structure analysis (FT-IR spectra) measurements, magnetic properties, Curie temperature, electric conductivity and dielectric properties for the mixed prepared *Ni-Zn* spinel ferrite " $Ni_{1-x} Zn_x Fe_2 O_4$ ".

4-2 Fourier transform infrared analysis (FT-IR spectra) measurements

In order to confirm the formation of the spinel structure, the FT-IR spectra of the ferrite samples were used. This is a very useful technique to describe the structural properties of the mixed ferrites. It would give information about the positions of the ions in the spinel lattice crystal, and their vibration modes. The vibration spectra can be indicated to the valance state of the ions, and their occupation in the spinel lattice crystal. The IR spectra absorption bands mainly appear due to the vibrations of the oxygen ions with the cations producing various frequencies of the unit cell.

In a certain mixed spinel ferrites, as the concentration of the divalent metal ions increasing, it gives rise to the structural change in spinel lattice crystal without affecting the spinel ferrite structure [58]. The structural changes brought about by the metal ions that are either lighter or heavier than divalent ions in the ferrites which strongly influence the lattice vibrations. The vibration frequency depends on the cations mass, the cations oxygen distance and the bonding–force [59].

The FT-IR spectra of the spinel structure of $Ni_{1-x} Zn_x Fe_2 O_4$ in the range 350 - 1000 cm^{-1} were recorded and shown in Fig. (4-1). The values of the absorption bands frequency are given in table (4-1). It shows that, the higher absorption bands tetrahedral band ν_T ranging from 600 cm^{-1} to 550 cm^{-1} and the lower absorption bands octahedral band ν_O at round 400cm^{-1}.This indicates that the spinel structure in the studied composition exists, and in a good agreement with the observation by many researchers for various ferrite materials [60-62].
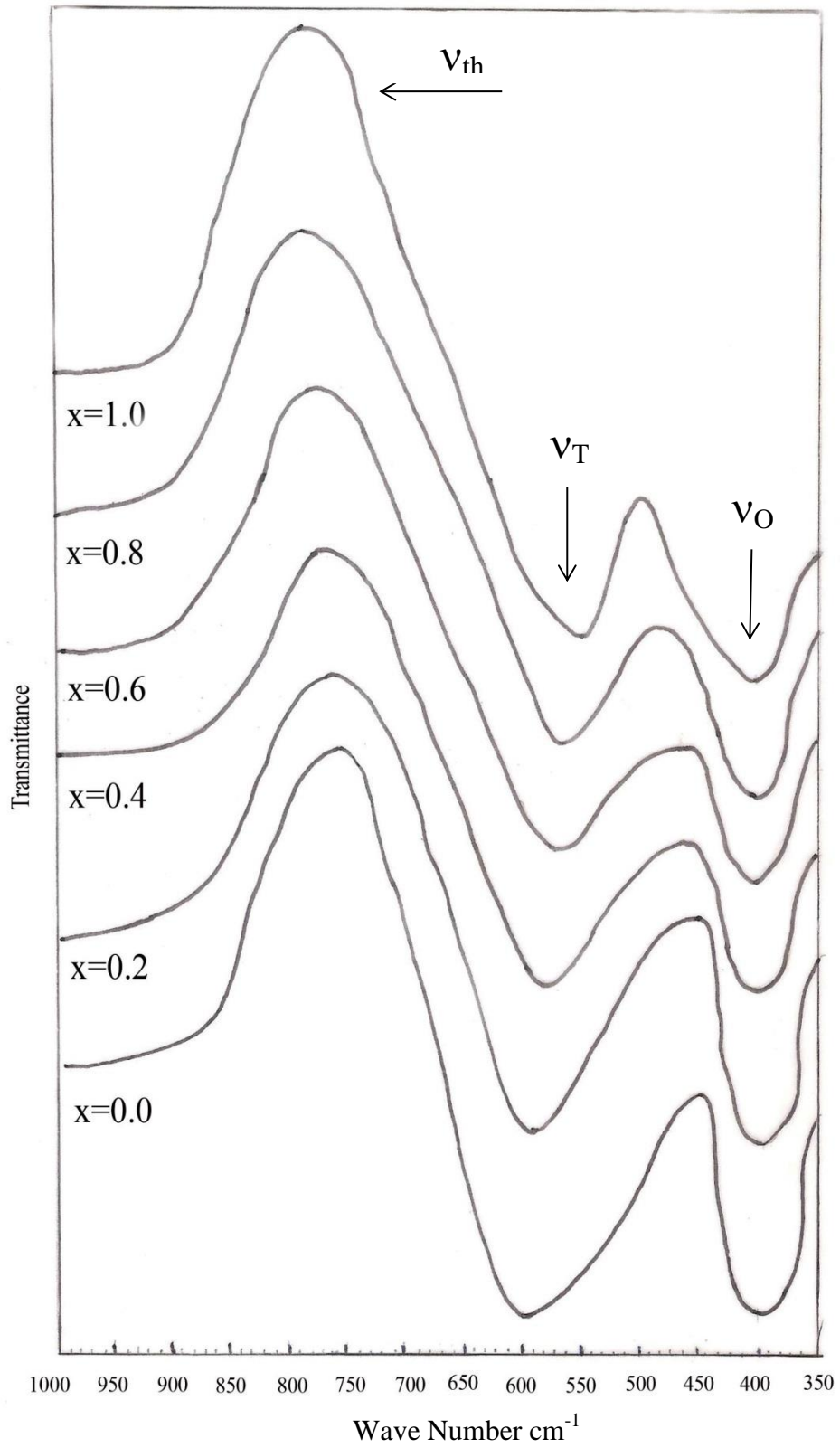
Fig.(4-1) FT-IR absorption spectra of the mixed Ni –Zn spinel ferrite.

As is also shown, the higher band ν_T is caused by the stretching vibrations of the tetrahedral metal- oxygen bonds Fe^{3+}- O^{2-}. Whereas, the lowest band ν_O is caused by the metal- oxygen vibrations in the octahedral sites as investigated in [60]

Table (4-1):Absorption bands frequency for the tetrahedral T_d , the octahedral O_h sites and values of ν_{th} for the mixed *Ni-Zn* spinel ferrite.

x	T_d **sites**	O_h **sites**	
	$\nu_T cm^{-1}$	$\nu_O cm^{-1}$	$(\nu_{th})cm^{-1}$
0.0	600	400	755
0.2	590	400	760
0.4	580	400	765
0.6	570	400	770
0.8	560	400	775
1.0	550	400	780

Fig. (4-2): Behavior of the absorption bands ν_T and ν_O with the Zn ratio" *x*"

Referring to table (4-1) and figure (4-2) it is noticed that, ν_T shifts to the lower frequency with increasing of the Zn^{2+} ions. The same behavior was reported in previous work of different ferrite systems [63,64]. A difference in the band position of ν_T was in the range from 600 cm^{-1} to 550 cm^{-1}, while ν_O has a constant 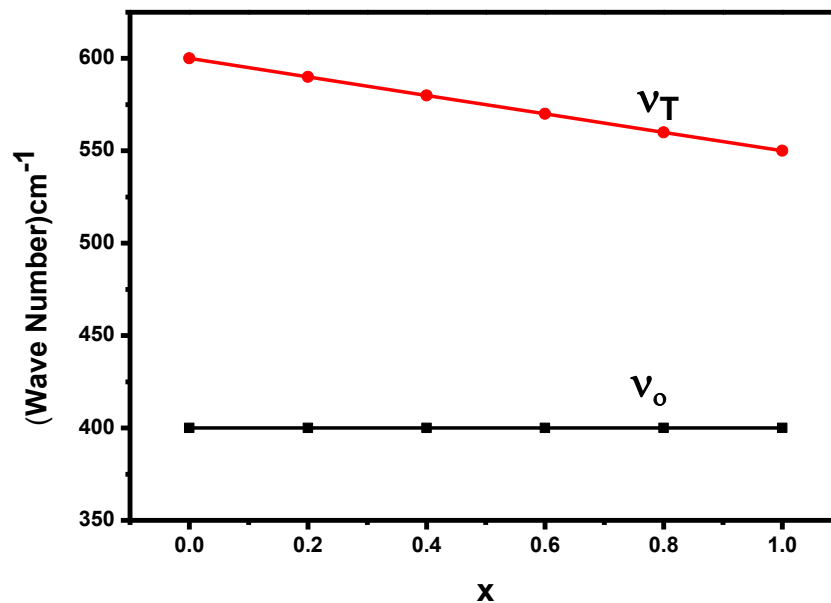value 400cm^{-1}. This is expected because of the difference in the $Fe^{2+} - O^{2-}$ bond distance for the T_d and the O_h complex [16,60,63,65]. It was also found that, the $Fe^{2+} - O^{2-}$ bond distance of the T_d sites (0.189 nm) and this is smaller than that of the O_h sites (0.199nm) [66]. This has been interpreted due to the more covalent bonding of the Fe^{3+} ions at the T_d sites.

Since the applied vibration frequency is proportional to the force constant F_C, so ν_T shift of the $Fe^{2+} - O^{2-}$ bond vibration to lower frequency with increasing of the Zn^{2+} ions. This indicates that, F_C of the $Fe^{2+} - O^{2-}$ bond decreasing in the mixed *Ni-Zn* spinel ferrite. The calculated values of the force constant F_{CT} and F_{CO} for the T_d and the O_h sites, respectively, are listed in table (4-2) using following relation [63]

$$F_C = 4\pi^2 c^2 \nu^2 m \qquad (4\text{-}1)$$

where

c is the light velocity $\approx 2.99 \times 10^{10} cm.\sec^{-1}$.

ν is the vibration frequency of the T_d and the O_h sites.

m is the reduced mass for the Fe^{2+} ions and the O^{2-} ions, it is found equal $\approx 2.061 \times 10^{-23} gm$.

Table (4-2): **Calculated values of the force constant F_{CT} and F_{CO} for the mixed *Ni-Zn* spinel ferrite.**

x	F_{CT} (*Newton.m^{-1}*)	F_{CO} (*Newton.m^{-1}*)
0.0	261.475	116.267
0.2	252.832	116.267
0.4	244.334	116.267
0.6	235.982	116.267
0.8	227.774	116.267
1.0	219.712	116.267

The FT- IR spectra of the composition $Ni_{1-x}Zn_xFe_2O_4$ shows a change in the absorption bands by introducing the Zn^{2+} ions, which has larger ionic radius and higher atomic weight, on the T_d sites. This tends to increase the ionic radius of the T_d sites with addition of the Zn^{2+} ions [65]. This is attributed to the method of preparation, the grains size and the porosity that influences the band position [16,58,60]. This affects the $Fe^{2+}-O^{2-}$ bond stretching vibration [46]. Therefore, there are slight shifts towards low frequency side in the v_T band.

The threshold frequency (v_{th}), according to Waldron [60] for the electronic transition can be determined from the maximum point in the absorption spectra, where it reaches a limiting value as in figure (4-1). Table (4-1) gives the v_{th} values and figure (4-3) shows the change of v_{th} as a function of the composition x. It is noticed that, the value of threshold frequency v_{th} is increasing with the increase of Zn content . This increment in v_{th} is not reflected on the value of the corresponding activation energy E_a. Which is calculated from the relation $E_{th}=hv_{th}$.
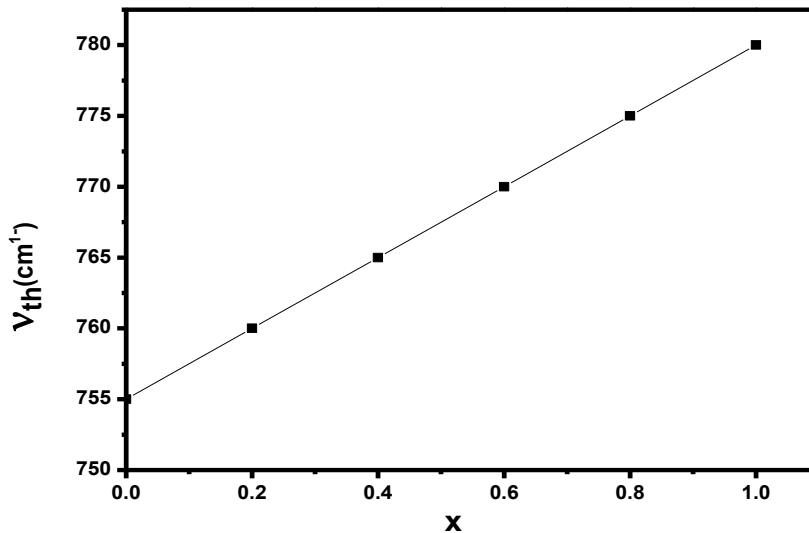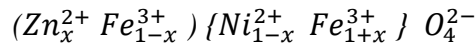

Fig. (4-3): Variation of v_{th} with the Zn ratio" x "

It is necessary to know the cations distribution, which could be described with the following considerations.

$$(Zn_x^{2+} Fe_{1-x}^{3+}) \{Ni_{1-x}^{2+} Fe_{1+x}^{3+}\} O_4^{2-}$$

The non-magnetic Zn^{2+} ions occupy the T_d sites, which are favored by the polarization effect and this occurs by replacing the Fe^{3+} ions in the T_d sites. However, the T_d sites preferences of the cations depend upon their electronic configuration [67]. The Zn^{2+} ions show a marked stronger preference for the T_d sites than the Fe^{3+} ions, where their (4s 3d) electrons form a covalent bonds with 2p electrons of the oxygen ion [68,69].

To calculate the ionic radius for the T_d and the O_h sites, we used the following equations [70,71]

$$R_T = \mathrm{x}R_{Zn^{2+}} + (1-\mathrm{x})R_{Fe^{3+}} \tag{4-2}$$

$$R_O = \frac{1}{2}[(1-\mathrm{x})R_{Ni^{2+}} + (1+\mathrm{x})R_{Fe^{3+}}] \tag{4-3}$$

where

R_T and R_O are the mean ionic radii per molecule for the T_d and the O_h sites, respectively.

$R_{Zn^{2+}}$ is the ionic radius of the Zn^{2+} ion

$R_{Fe^{3+}}$ is the ionic radius of the Fe^{3+} ion

$R_{Ni^{2+}}$ is the ionic radius of the Ni^{2+} ion.

The ionic radii R_T and R_O versus the Zn ratio" x "are plotted in figure (4-4), while R_T/R_O versus the Zn ratio" x" is plotted in figure (4-5). clearly, it is noticed that, R_T increases while R_O decreases with increasing of the Zn^{2+} ions. This behavior is attributed to the replacement of the Fe^{3+} ions with the larger ionic radius of the Zn^{2+} ions on the T_d sites and the Ni^{2+} ions with the smaller ionic radius of the Fe^{3+} ions on the O_h sites.

Table (4-3): Values of R_T , R_O and R_T/R_O for the mixed *Ni-Zn* spinel ferrite

x	R_T(nm)	R_O(nm)	R_T/R_O
0.0	0.063	0.076	0.82894
0.2	0.0652	0.0746	0.87399
0.4	0.0674	0.0732	0.92076
0.6	0.0696	0.0718	0.96935
0.8	0.0718	0.0704	1.01988
1.0	0.074	0.069	1.07246
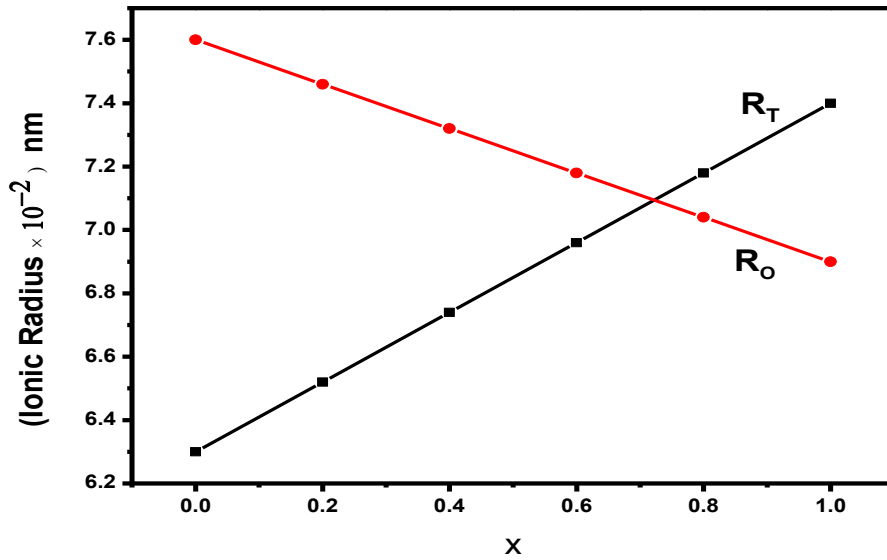
Fig. (4-4): Variation of R_T and R_O with the Zn ratio" *x*"
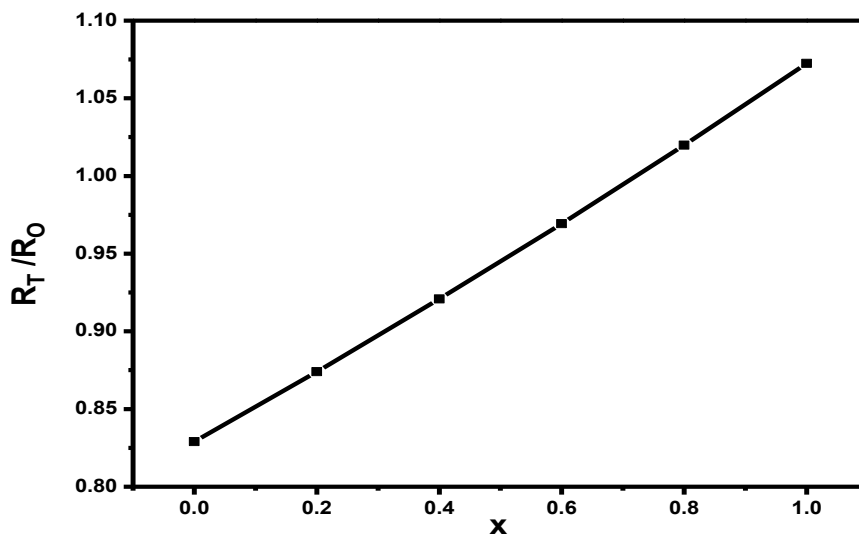

Fig. (4-5): Variation of R_T/R_O with the Zn ratio" *x*".

52

4-3 *Magnetic Properties*

4-3-1 Magnetization Study

The relation between the net magnetization M ($A.m^{-1}$) and the applied magnetic field intensity H ($A.m^{-1}$) for the ferrite samples of the system $Ni_{1-x} Zn_x Fe_2O_4$ were studied at room temperature "300K". The obtained results for all the ferrite samples were illustrated in figure (4-6),where the variation of M and H for the samples with different composition plotted .

In the range of the applied magnetic field H of (0-3500 $A.m^{-1}$), the measured net magnetization M ($A.m^{-1}$) of the samples does not exhibit a saturation magnetization. The saturation magnetization of a mixed Zn spinel ferrite at the absolute zero point would be expected to increase with increasing of the Zn^{2+} ions.Thus, the remarkable fact appears that, the substitution of the magnetic ions in a ferrimagnetic materials by the non-magnetic such Zn^{2+} and Cd^{2+} ions can lead to an increase in the saturation magnetization[13].

When the concentration of Fe^{3+} ions in the tetrahedral sites A site is diluted by low concentration of diamagnetic substances such as Zn^{2+} ions, net magnetization increases.

This behaviour was shown for the samples of $x \leq 0.6$ as shown in figure(4-7). However magnetization decreases when Zn contents is increased   as Zn^{2+} ions increase for the samples of ≥ 0.8. The reason for this nature is that low Zn^{2+} concentration reduces the number of spins occupying the tetrahedral sites A site in the sublattice, causing the net magnetization increases. As the Zn^{2+}content increases more, the exchange interactions are weakened and the B site spins octahedral sites are no longer held rigidly parallel to the few remaining A site spins tetrahedral sites. The decrease in B site Sublattice moment , interpreted as spin departure from co-linearity causes the effect known as canting, this effect also described in samples of Cu-Zn ferrite[72].

From figure (4-**7**), it is noticed that, the value of magnetization increases with increasing of the Zn^{2+} ions, gradually from $x = 0$ and reaches to the maximum value for $x = 0.6$ with composition $Ni_{0.4} Zn_{0.6} Fe_2O_4$, and then decreases gradually

with an increase of Zn^{2+} composition . This indicates a very low net magnetization at the samples with $x \geq 0.8$. The obtained results agreed well with the results obtained earlier [47,73-76] .

The increase of the net magnetization when the Zn^{2+} ions are increased can be explained by Neel's two-sublattice model of the magnetism theory of the ferrimagnetic materials [71] . Also, the drop in the net magnetization for samples with $x \geq 0.8$ is due to the occurrence of the non-collinear spin structure. As a result, some sort of triangular, antiferromagnetic, or other spin arrangements occur within the O_h sublattice and therefore the net moment decreases. This could not be explained on the basis of Neel's two-sublattice model, but by the three-sublattices model that was suggested by Yafet and Kittel [46,77,78].

Owing to the presence of the non-magnetic Zn^{2+} ions at the tetrahedral T_d sites, the net magnetization of the T_d lattice will be smaller than in the simple ferrite, since, the Fe^{3+} ions have the largest magnetic moment are positioned at the O_h sites. When the Zn^{2+} ions increase the cations distribution is not altered, but the exchange interaction between the tetrahedral T_d and the octahedral O_h sublattices getting weakened. However, the exchange interaction between O_h and O_h sublattices go through a change in its tendency from ferrimagnetic state to antiferromagnetic state [46,49]. This behavior is related to the increase of the non-magnetic ions Zn^{2+} ions in the ferrite compositions. Previous studies [45,48] and Chinnassamy [79] mentioned that, Zn spinel ferrite in the bulk form gives a normal spinel ferrite with the Zn^{2+} ions at the T_d sites, while the Fe^{3+} ions at the O_h sites.
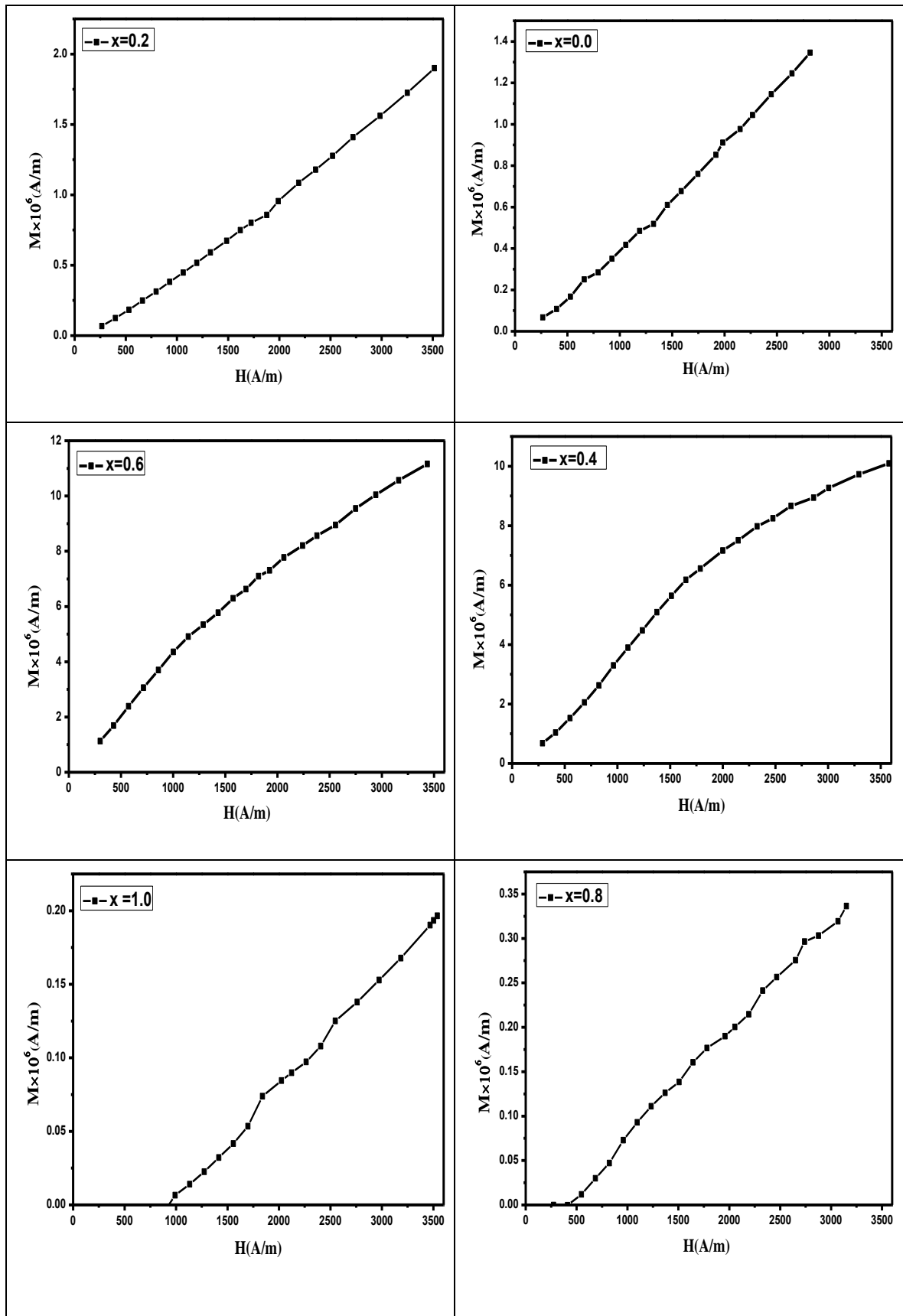
.

Fig. (4-6): Variation of M **with** H **for the samples with** x = 0.0, 0.2, 0.4 0.6 ,0.8 and1.0 .
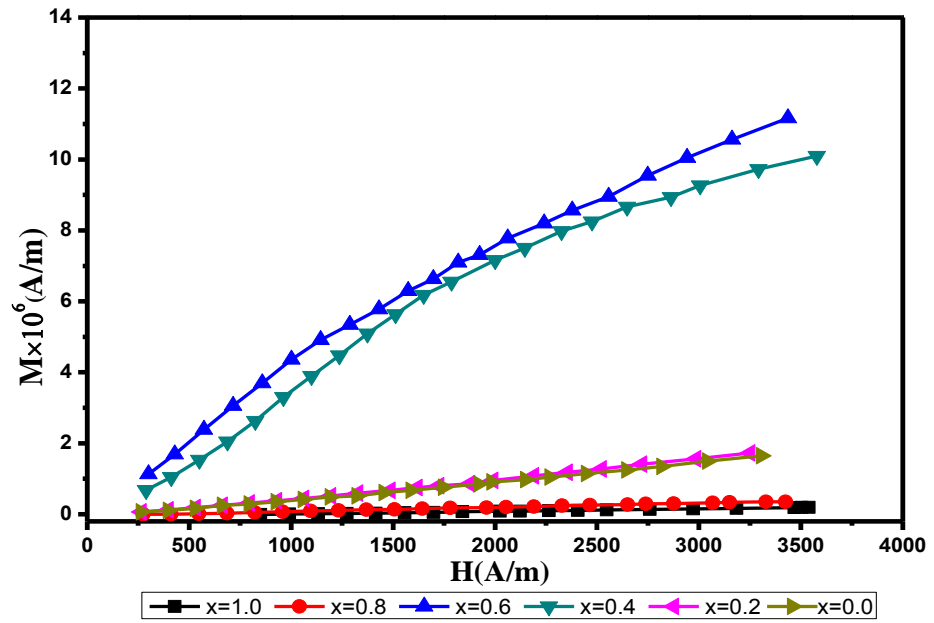
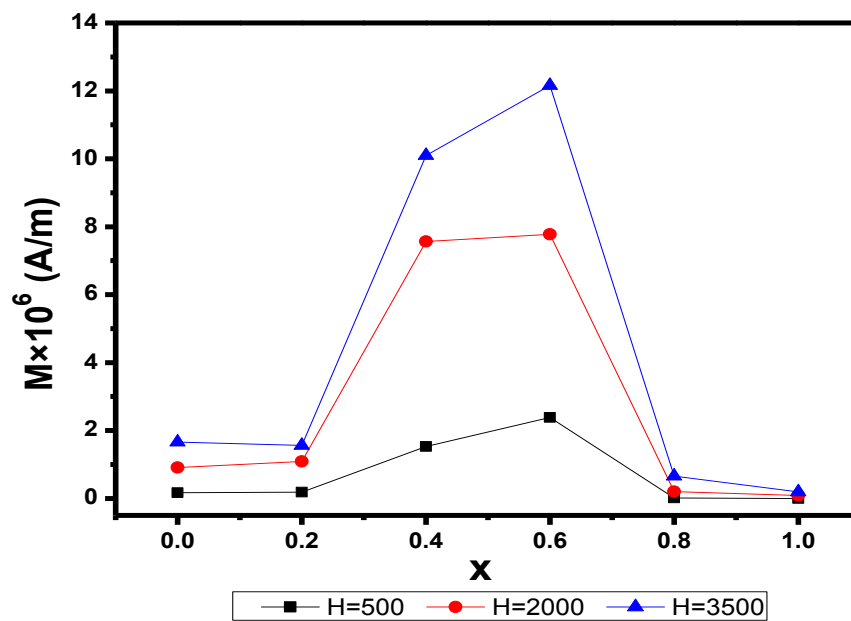**Fig. (4-7): Variation of *M* with *H* for all the samples , for different compositions**

Fig. (4-8) : Variation of *M* with the composition *x* for different values of *H* (A.m^{1-}).

4-3-2 Magnetic Moment

The net magnetization M_{net} for the ferrimagnetic materials defined with the individual magnetization, M_T of T_d and M_O of O_h sublattices. Since the net magnetization M_{net} cannot be observed, it is defined by the net magnetic moment μ_{net} per unit volume for each sample in Bohr magnetos unit. The μ_{net} is calculated according to the cations distribution for the mixed *Ni-Zn* spinel ferrite formula, in which tetrahedral sites are occupied by Zn^{2+} and Fe^{3+} ions, and the octahedral sites are occupied by Ni^{2+} and Fe^{3+}. The results have a good agreement with the cations distribution, that suggested by several authors [2, 3,6,46].

$$(Zn_x^{2+}\ Fe_{1-x}^{3+})\ \{Ni_{1-x}^{2+}\ Fe_{1+x}^{3+}\}\ O_4^{2-}$$
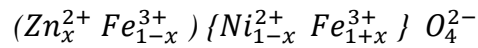
The net magnetic moment μ_{net} in the spinel structure is equal to the different moments from the tetrahedral and octahedral sites ,which are given by [3,5]

$$\left|\vec{\mu}_{net}\right| = \left|\vec{\mu}_o\right| - \left|\vec{\mu}_T\right| \tag{4-1}$$

According to the cations distribution form, the magnetic moment for the T_d sites, μ_T and the O_h sites, μ_O , were calculated using the following equations [3,5]

$$\mu_T = 2(1-\mathrm{x})S_m\mu_B \tag{4-2}$$

$$\mu_O = [(1-\mathrm{x})S'_m + (1+\mathrm{x})S_m]2\mu_B \tag{4-3}$$

Where $S_m = 5/2$ is the spin quantum number of the Fe^{3+} ions , $S'_m = 1$ is the spin quantum number of the Ni^{2+} ions , and the Zn^{2+} ions are diamagnetic ions which has zero spin quantum number. Therefore, the net magnetic moment in the spinel structure is enhanced with the zinc concentration , for the sample $ZnFe_2O_4$ at *x*=1.0 which represents a high concentration of zinc . In this sample , the zinc ions weakens the super-exchange interaction between the magnetic ions, so $ZnFe_2O_4$ represents an antiferro-magnatic characteristic.

The calculated values of μ_T , μ_O and μ_{net} are listed in table (4-4) and their variation with the composition *x* are represented in figure (4-9).

Table (4-4): Calculated values of μ_O, μ_T and μ_{net} according to the cations distribution of the mixed *Ni-Zn* spinel ferrite.

x	$(\mu_O)\mu_B$	$(\mu_T)\mu_B$	$(\mu_{net})\mu_B$
0.0	7	5	2
0.2	7.6	4	3.6
0.4	8.2	3	5.2
0.6	8.8	2	6.8
0.8	9.4	1	8.4
1.0	10	0	10
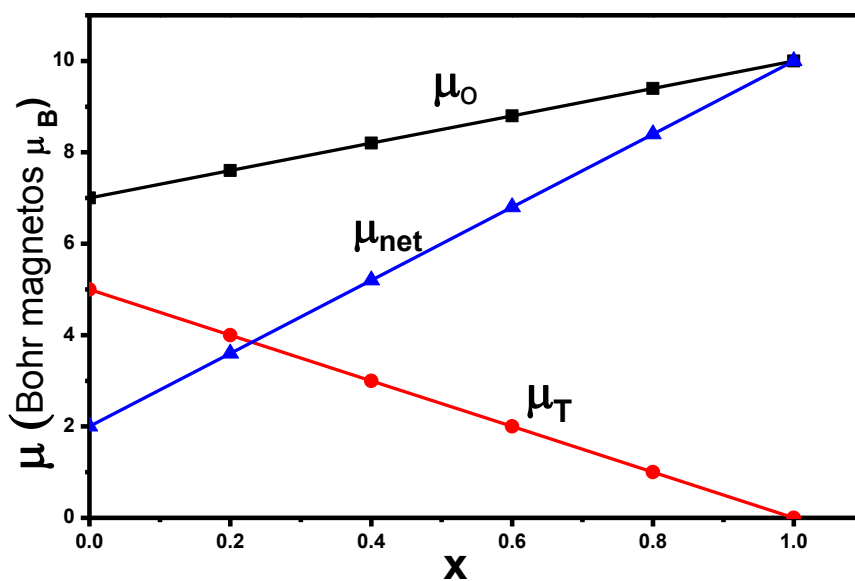
Fig. (4-9): Variation of μ_O, μ_T and μ_{net} with the Zn ratio" *x*".

It is clear that, as the composition x increased, both of μ_{net} and μ_O are increased, while μ_T is decreased.

The variation of the μ_{net} with the Zn^{2+} could be explained by assuming that, as the concentration of Zn^{2+} increased the relative number of the Fe^{3+} ions increased on the O_h sites, and decreased on the T_d sites. This tends to increase μ_O and decrease μ_T. Therefore, the μ_{net} would rise linearly with the Zn^{2+} ions and would reach value $10\mu_B$ per molecule might be expected on $x = 1.0$, when all the divalent magnetic ions have been replaced by the Zn^{2+} ions.

4-3-3 Relative permeability

The relative permeability μ_r for all samples gives the description of the magnetization behavior during the change of the exposed external applied field. It is defined as the ratio between the induction field B and the intensity of the applied magnetic field H, and defined as $\mu_r = B/\mu_o H$. The relation between H and μ_r has an interesting behavior for the present ferrite samples as shown in figure (4-10).

The increase of magnetic field intensity H causes pronoucend increase of μ_r which decrease with increasing of Zn^{2+} content (low spin ion). The increment of μ_r could be related to the alignment effect of H on the ionic spins. In such away, the increase H causes rapid increasing of B, which causes increasing of μ_r ,the maximum value of μ_r is found for the sample of x =0.6 with composition $Ni_{0.4}Zn_{0.6}Fe_2O_4$.

Figure (4 -10) also showed that for the samples with $x=0.6$ and $x=0.4$ μ_r increases with increasing H till a maximum value , after this value it decreases, this decrement of μ_r for these two samples is more pronounced than the rest of the examined samples. This means that these two samples have the highest spin ordering (highest intrinsic magnetization) compared with the other samples. It is also noticed that, the ionic ordering of these two samples is closer to the saturation state than the others. Accordingly, the increase of H might cause a slight increase of B giving rise to a distinct decrease in μ_r . However, figure (4 -10) showed that the samples with $x \geq 0.8$ have the smallest value of μ_r . This behavior is attributed to that these two samples have very low magnetization.
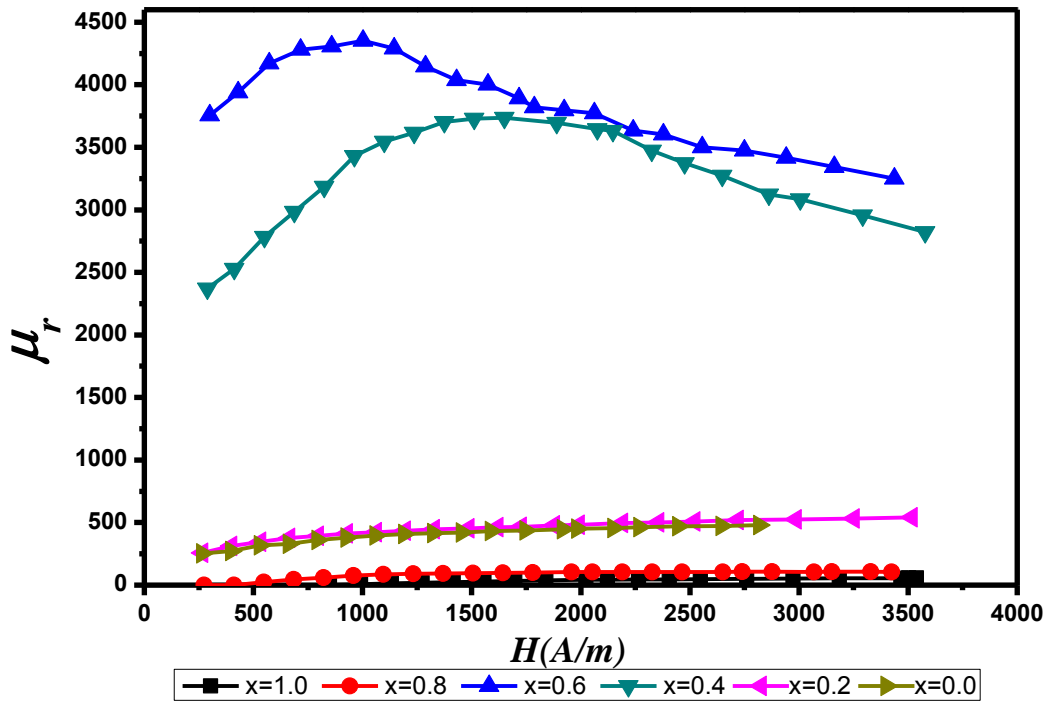
Fig. (4-10): Variation of μ_r with H for all the samples with differnet composition x=0.0,0.2,0.4,0.6,0.8and1.0

4-4 Electrical Properties

4-4-1 DC Conductivity and Curie point (T_C)

The temperature dependence of electrical conductivity of mixed Ni-Zn ferrites of different compositions has been investigated from room temperature to fit beyond the curie temperature.

The variation of $\ln(\sigma_{DC})$ against the reciprocal of temperature ($10^3/T$) is depicted in figure (4-11). From this figure it is seen that, $\ln(\sigma_{DC})$ continuously increases with the increasing the temperature. This conforms that the ferrite under various ferrite systems [50,80-82].

Fig (4-12) gives a plot of $\ln(\sigma T)$ versus ($10^3/T$). It can be seen that the value of $\ln(\sigma T)$ increases linearly with temperature up to a certain temperature T_c at which a change of slope has occurred. The transition temperature T_c which are given in table (4- 5) along with the values of Curie temperature. It is observed from the table that the transition temperature T_c is in a good agreement with the Curie temperature showing that the change in the slope in each case has occurred at Curie point of the corresponding ferrite. Similar transitions in the neighborhood of the Curie have also been observed by several investigators in various ferrite systems. [83,84]

It was shown theoretically that on passing through the Curie point a change must occur in the gradient of the straight line and the magnitude of the effect depends on the exchange interaction between the outer and the inner electrons which alter the Curie point .
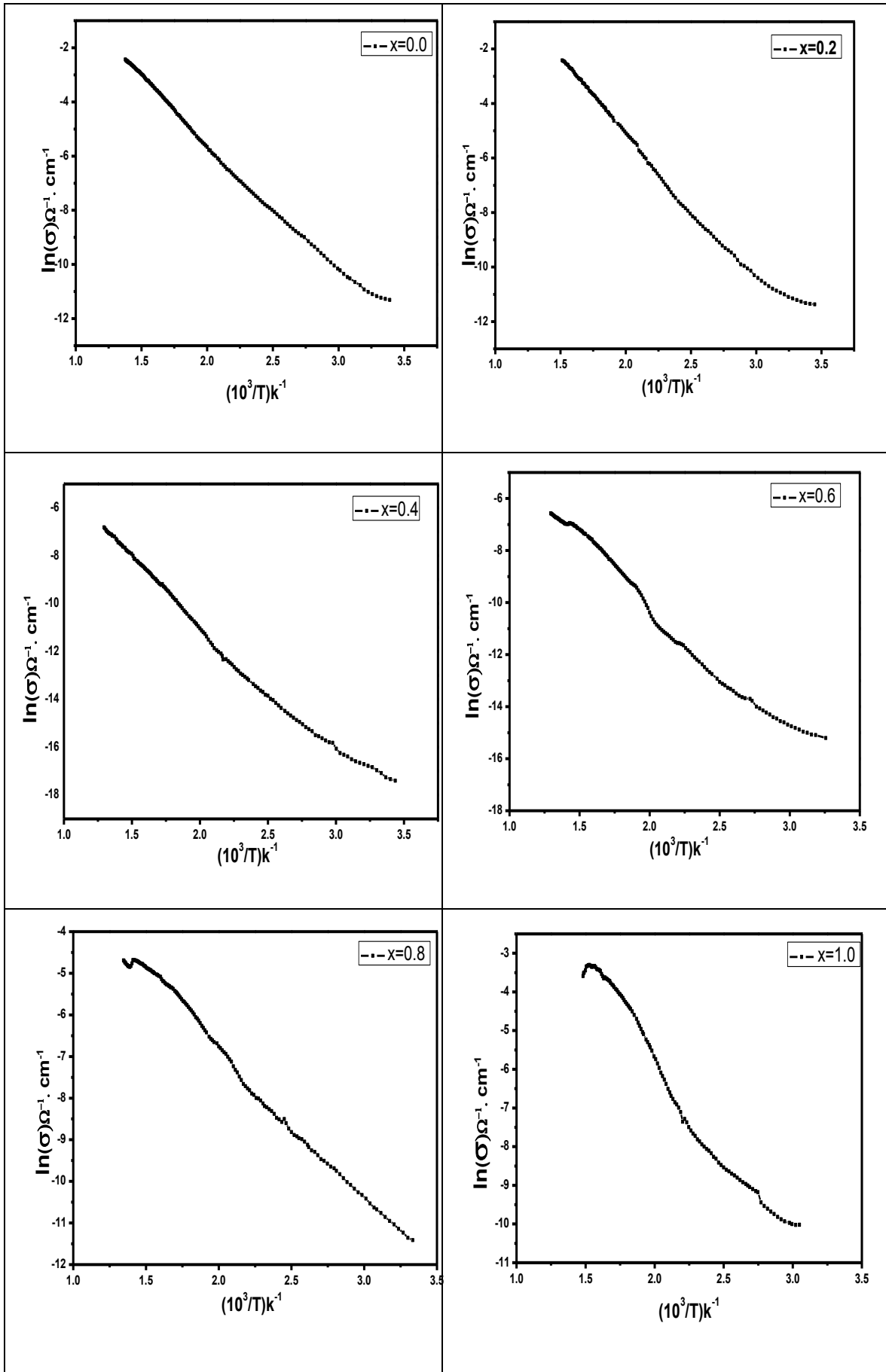
Fig. (4-11): Variation of ln σ$_{DC}$ with $(10^3/T)$ for all the samples.

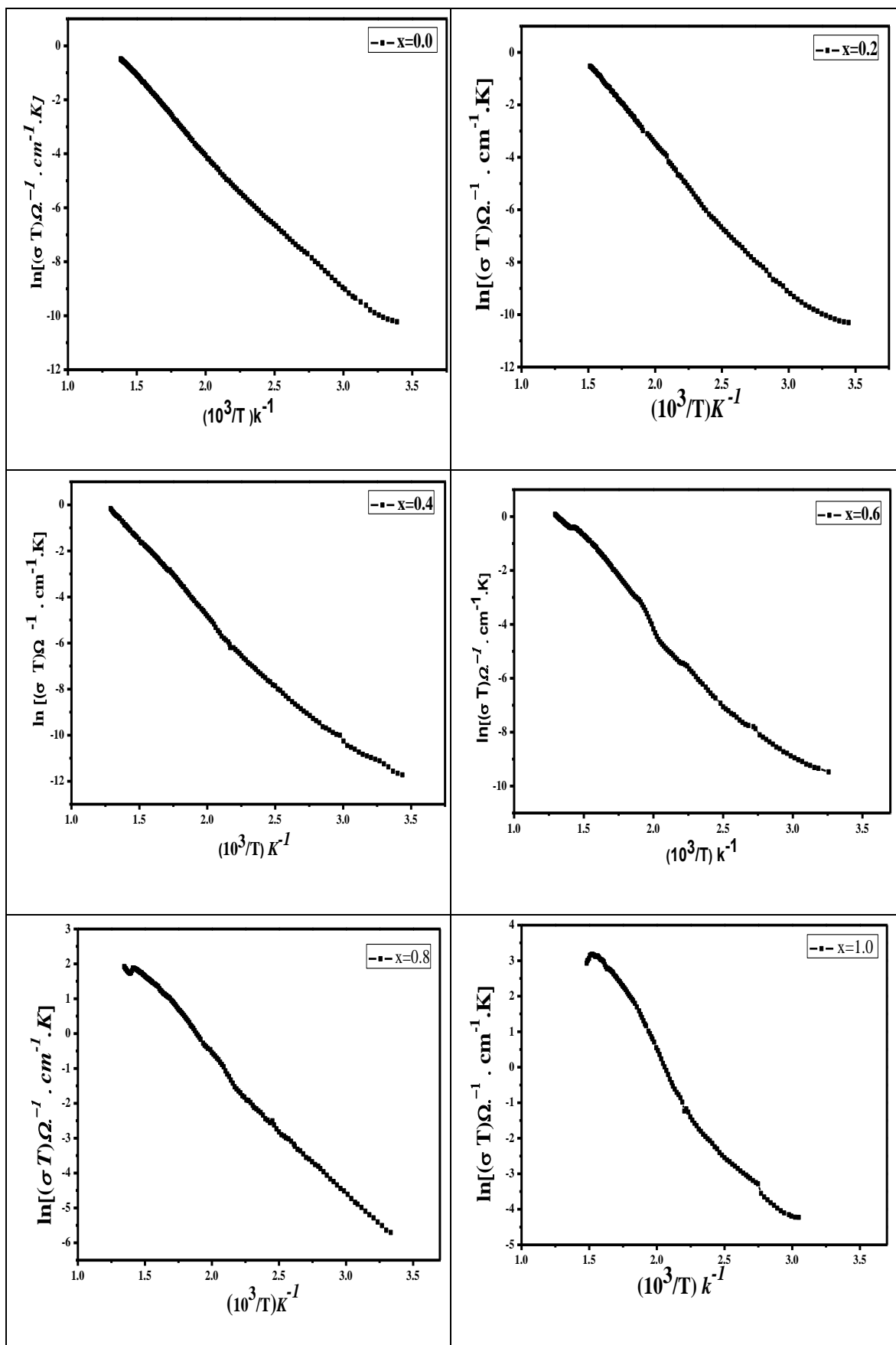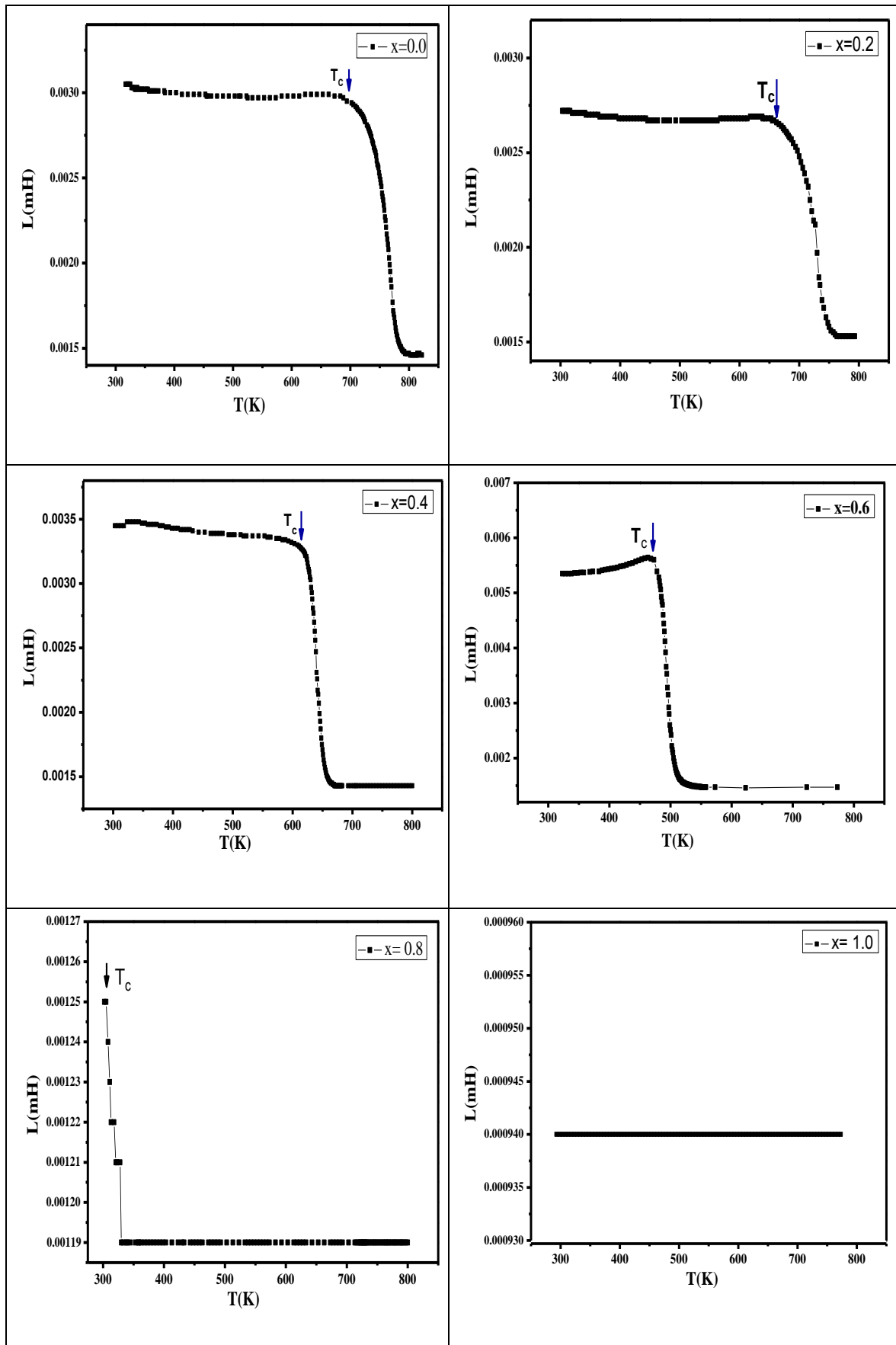**Fig. (4-12): Variation of ln(σ T) with ($10^3/T$) For the samples with x=0.0,0.2,0.4, 0.6,0.8and1.0**

Fig. (4-13): Variation of inductance L with temperature T for all the samples with differnet composition x=0.0,0.2,0.4,0.6,0.8and1.0.

Table (4-5): Values of T_C which determined by the induction measurements and the DC conductivity measurements for the mixed *Ni-Zn* spinel ferrite.

x	induction **Results** $(T_C)K$	**DC** conductivity **Results** $(T_C)K$
0.0	694	641
0.2	658	666
0.4	619	624
0.6	468	458
0.8	302	-
1.0	-	-

The DC conductivity is useful to calculate the different activation energies for the given ferrite system from the slope of the figure (4-12), activation energy of the samples was determined and listed in table (4-6). The calculated values for both ferrimagnetic and paramagnetic activation energy ΔE for the studied compositions were calculated . The values of activation energy ΔE in paramagnetic region found to be greater than those observed in ferrimagnetic region. The decrease in activation energy may be due to the decrease in resistivity with increasing Zn^{2+} concentration because activation energy behaves in the same way as resistivity [85,86].

Generally the change of slope is attributed to change in conductivity mechanism. The conduction at a lower temperature (below Curie temperature) is due to hopping of electrons between Fe^{2+} and Fe^{3+} ions, whereas at a higher temperature (above Curie temperature) due to hopping of polarons.[87,88] .

The dependence of the *DC* conductivity on temperature in the figure (4-13) fulfils the relation [5]

$$\sigma = \frac{S'''}{T} e^{(-E_a/kT)}$$

(4-5)

here *S''* is a constant given by ($ne^2d^2 v/k$) [85],where :

d : is the distance between the nearest neighbor cations

v : is the frequency of the vibration of the crystal lattice

n : is the number of the charge carriers.

Table (4-6): Values of the ferrimagnetic activation energy E_f and paramagnetic activation energy E_p

x	Activation Energy	
	$(E_f)eV$	$(E_p)eV$
0.0	0.32	0.43
0.2	0.28	0.35
0.4	0.21	0.28
0.6	0.17	0.20
0.8	-	-
1.0	-	-

4-4-2 Inductance

Inductive sensing is based on measuring the variation of inductance L of the toridial shape specimens for all samples of Ni-Zn ferrites .The variation of the inductance L has been investigated from room temperture to fit beyoud the Curie temperture . Figure (4-13) gives aplot of the inductance versus T (k). It can be seen that the value of inductance L is constant with temperture up to acertain temperture T_c at which a sharp drop of the value of L is occurred, at this value of temperture and the transition in the sample has occurred. The transition temperture T_c which are given in table (4-5) along with the value x of Curie temperture T_c were detrmined. It is observed from the table that the curie temperture is decreased with increasing Zn content and it was found that the sample of x=1.0 has no transition since it is paramagnatic at room temperture as seen in fig (4-13). While T_c , for all other sample has occured , that the sample under investigation has transition from ferrimagntic at lower temperture " below curie temperture "and paramagntic at higher temperture "above currie temperture" as indicated in fig (4-13) and table (4-5) . It is found that the transition temperture decreased as the Zn content increased.

As shown in the table (4-5), there is a small deviation of the T_C value from the induction measurements and the conductivity measurements. This indicates that, the magnetic transition can be manifested in the transport property. However, this

change of slope could not be observed in the composition with $x = 0.8$ and x=1.0, since the sample of x=0.8 has T_c at room temperature, while the sample of x=1.0 is considered diamagnetic materials at room temperature. The same behavior was shown in the *Cd* spinel ferrite which is found as the diamagnetic substance at room temperature [90].

The variation of Curie temperature with composition x was plotted in figure (4-14) . It shows that T_c decrease as x increased , for the sample of x=0.8 the T_c value is at room temperature " the lowest value of " T_c " .

As it was represented in figure (4-14), the T_C decreased continuously with increasing of the Zn^{2+} ions. This decrease in the T_C with increasing Zn^{2+} ions on the ferrimagnetic materials was, also, observed by other workers [91-92]. This is attributed to the addition of the non-magnetic Zn^{2+} ions that replaced the magnetic Fe^{3+} ions at the T_d sites, thus; the number of the Fe^{3+} ions decrease at the T_d sites. This tends to decrease the strength of T_d and O_h exchange interactions of the type $Fe_T^{3+} - O^{2-} - Fe_O^{3+}$, apart from decreasing number of bonds or linkages between the magnetic ions [93].
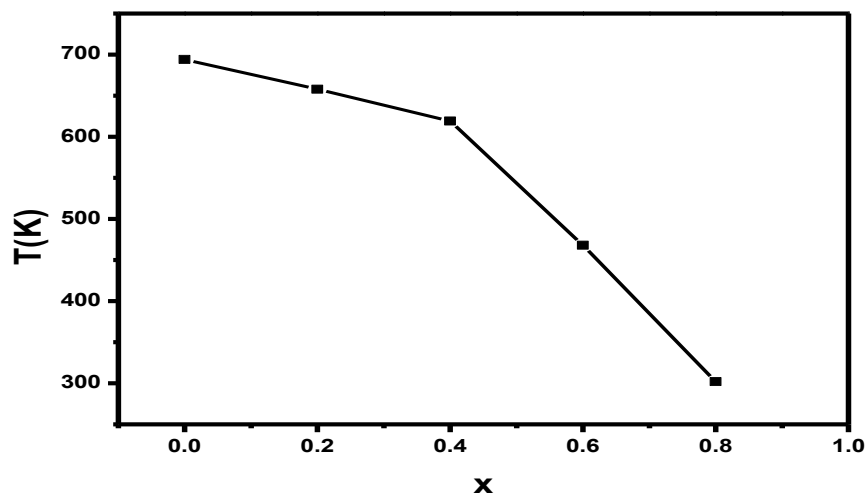

Fig. (4-14): Variation of T_C with Zn ratio "x".

4-5 Dielectric Properties

Dielectric properties such as dielectric constant ε and dielectric loss tangent $\tan(\delta)$ has been investigated in the frequency range $10^4 Hz$–$10^6 Hz$ at room temperature for the given mixed *Ni-Zn* spinel ferrite. The variation of these parameters with composition x and frequency is explained qualitatively. The variation of the dielectric constant ε verses frequency is represented in figure (4-15) . Also, The variation of the dielectric loss tangent $\tan(\delta)$ verses frequency represented in figure (4-16).

Theoretically, to find the relation of ε and $\tan(\delta)$ with the applied frequency from equation [11]

$$\varepsilon \tan(\delta) = \frac{\sigma_{AC}}{\nu} 1.8 \times 10^{10}$$

(4-4)

The above equation predicts that, ε and $\tan(\delta)$ is inversely proportional to the applied frequency. The general trends for all compositions is that, ε and $\tan(\delta)$ were found to decrease continuously with increasing of the applied frequency and showed normal dielectric behavior of the spinel ferrite. This behavior was, also, observed in various ferrite systems [51,52,94,95].

The same figures show that the value of ε and $\tan(\delta)$ decreases continuously with increasing frequency. The decrease in the value of dielectric constant ε and loss tangent $\tan(\delta)$ as the frequency increases may be due to electron exchange interaction between the Fe^{2+} and the Fe^{3+} ions, which cannot follow the alternating electric field. A similar behavior was also observed in [96,97] of various ferrite systems .

The obtained results of the dielectric constant indicated that, the sample of x=1.0 with composition $ZnFe_2O_4$ was given a maximum dielectric dispersion among all the component . A qualitative explanation can be given for the occurrence of the maximum in the $\tan(\delta)$ verses frequency curves in the case of mixed Ni–Zn ferrites. as pointed out by Iwauchi [98] .

There is a strong correlation between the conduction mechanism and the dielectric behavior of ferrites. The conduction mechanism in ferrites is considered as due to hopping of electrons between Fe^{2+} and Fe^{3+} situated on the octahedral sites O_h. This behavior of the dielectric properties can be explained qualitatively by the mechanism of the polarization process in the ferrites which is similar to that of the conduction process [98].
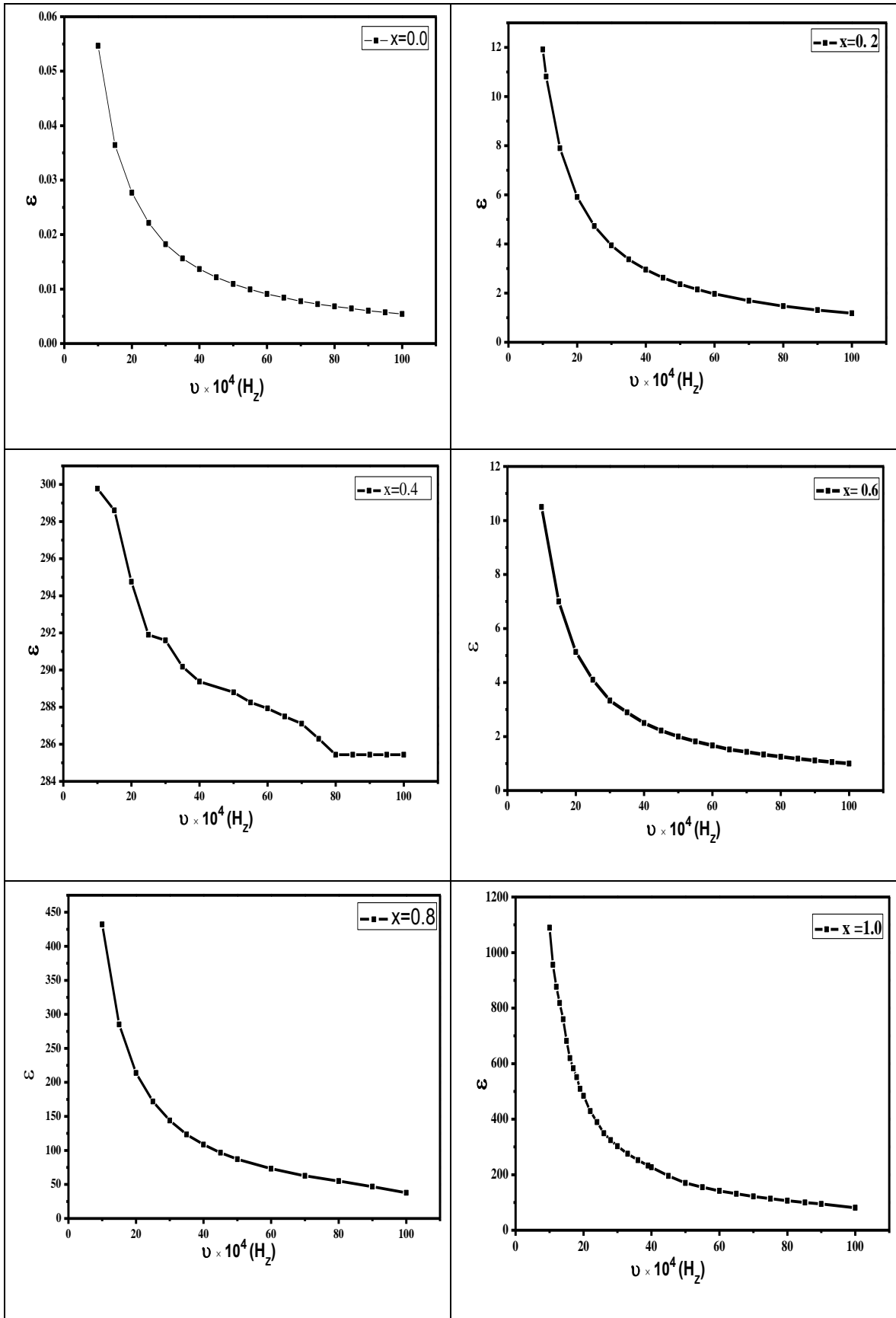
Fig. (4-15): A Plot of ε against the applied frequency for all the samples at room temperature.
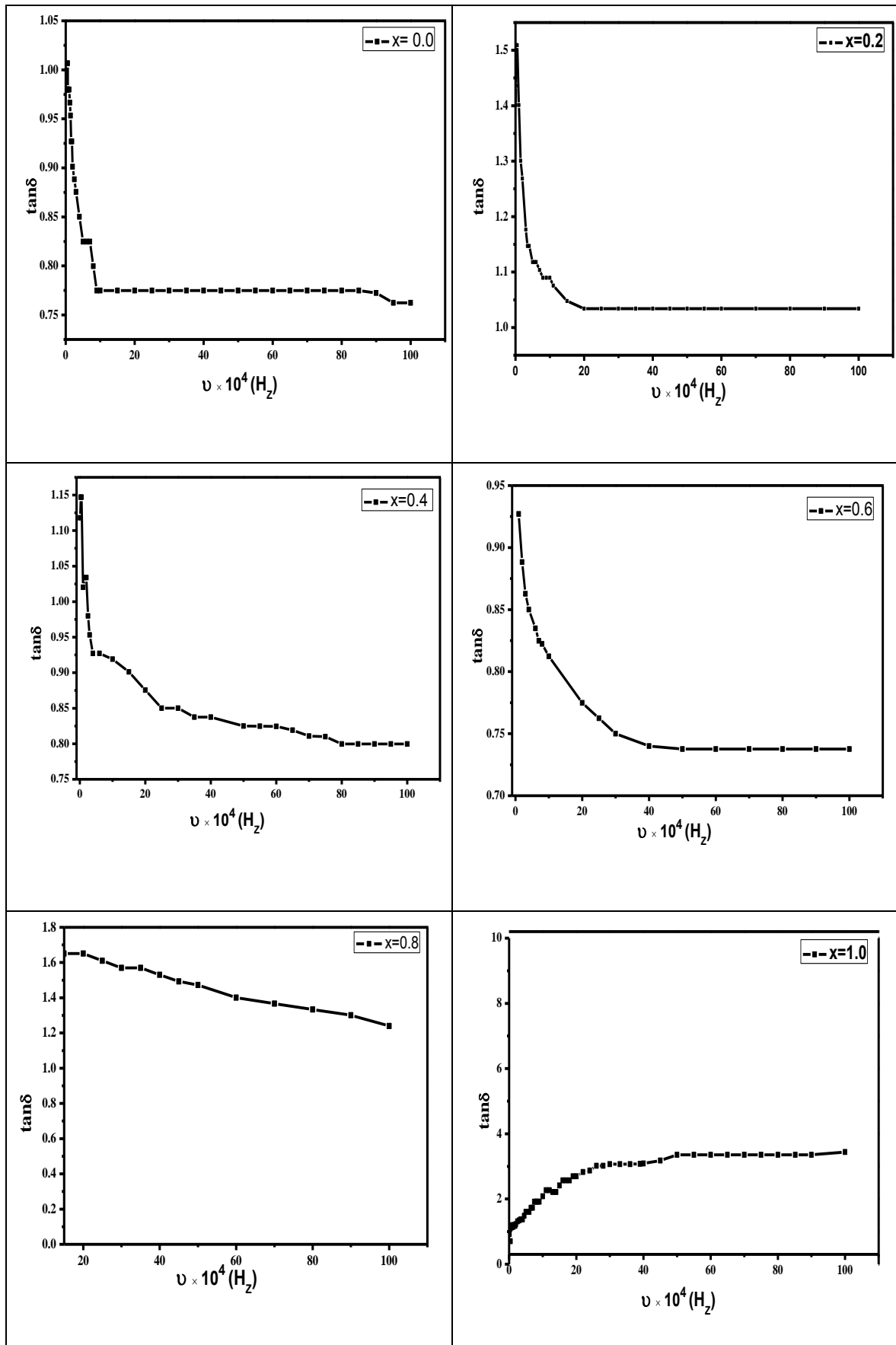
Fig. (4-16): A Plot of $\tan(\delta)$ against the applied frequency for all the samples at room temperature .

71

CONCLUSION

Substitution of the non-magnetic Zn^{2+} ions in *Ni* spinel ferrite has a tremendous influence such the structure of the samples, the magnetic properties, the electric properties and the dielectric properties. From this study we concluded from the obtained results that :

- Two mainly prominent bands were detected by using FT-IR spectra, one of high frequency band ν_T at round 600 cm^{-1} to 550 cm^{-1}, and another at low frequency band ν_O at round 400cm^{-1} were assigned to the tetrahedral sites T_d and the octahedral sites O_h, respectively. This indicated that the spinel structure is exist in investigated samples.

- The ionic radius of the tetrahedral sites T_d and the octahedral sites O_h sites calculated and they are changed linearly with increasing of the Zn^{2+} ions.

- The magnetization increased with increasing of the Zn^{2+} ions for the samples with x= 0.0 to x =0.6, then decreased for samples of x≥ 0.8 while Zn^{2+} content increase .

- The increasing of the magnetization was explained on the basis of Neel's two sublattices model. And the net magnetic moment was calculated for the T_d sites and the O_h sites, according to the suggestion cations distribution.

- From the DC conductivity, we concluded that the samples have the same behavior of semiconductor materials.

- The activation energy in paramagnetic region was higher than ferrimagnetic region. This attributed to the existence of polaron-hopping.

- The measuring of inductance indicate a good manur to determine Curie temperature points for all the samples and showed decreasing with increasing of the Zn^{2+} ions

- It can be seen that the value of inductance L is constant with temperature up to a certain temperature T_c at which a sharp drop of value L is occurred

- It is found that transition occurs for all samples except the sample with x=1.0 there is no transition, so it considered as a paramagnetic at room temperature.

- Dielectric constant and dielectric loss tangent were found to decrease for all samples with increasing of the applied frequency. This is attributed to a correlation between the conduction mechanism and the dielectric behavior of the ferrites .

Furthermore, Zn content has significant influence on the electromagnetic properties , such as dielectric constant , dielectric loss tangent, electrical properties and magnetic properties for Ni ferrites, so, the mixed Ni-Zn spinel ferrite is considered a soft ferrite material, which is proved to be an interest material for technological and scientific applications

REFERENCES

[1] M. N . Rudden and J. Wilson, "Elements of Solid State Physics". John Wiley and Sons. Ltd, (1984).

[2] S. Chikazumi, "Physics of Magnetism", New York, John Wiley and Sons. Inc., (1964).

[3] D. C. Tayal, " Electricity and Magnetism ", Hina Laya Publishing House(1998).

[4] Allan. H. Morrish, "The Physical Principles of Magnetism", John Wiley and Sons. Inc, (1965).

 [5] H. A. Dawond, "A study of Some Electric and Magnetic Properties of Li-Cu Spinel ", Pd.D. Thesis, Faculty of Science Zagazig University, (1997).

[6] J. Smit and H. P. J. Wijn, " Ferrites ", New York, John Wiley, (1959).

[7] E. C. Snelling, Proc. Brit. Ceramic Soc. Z. ,151, (1964).

[8] E. C. Snelling, " Soft Ferrites Properties and Applications ", London IIIFFE. Books Ltd. (1969)

[9] E. S. Albers. J. Appl. Phys., 25, 152, (1954).

[10] H. P. Peloschek, " Square Loop Ferrites and The Applications " , London, J.Birks and Hart Heywood and Co. Ltd. (1963).

[11] B. Lax and K. J. Button, " Microwave Ferrites and Ferrimagnetics " , Mc. Grow-Hill (1962).

[12] E. W. Gorter, Philips Res. Rept, 9, 295, (1954).

[13] E. J. W. Verwey and E. L. Helimann, J. Chem. a Phys., 15 , 4, (1947).

[14] E. J. W. Verwey, F. Deboer and J. H. Vansanten, , J. Chem. Phys, 16,12, (1948).

[15] C. Kittel, "Introduction to Solid State Physics", John Wily Sons, 5th Edition.

[16] O. S. Josyulu and J. S. Obhanadri, Phys. Stat. Sol. (A), 65, 479, (1981).

[17] M. C. Lovell and A. J. Avery, M. W. VerNon, "Physical Properties of Materials ", Van. Nonstrand Reinhold Company, (1976).

[18] John Crangle," Solid State Magnetism ", Edward Arnold, Adivision of Hodder, and Stonsghton, London, (1991) .

[19] Ferroxcube, " Soft Ferrite ", Jan. (2002).

[20] Raymond A.Serway, "Physics For Scientists and Engineers with Modren Physics", Saundres College Publishing, (1996).

[21] R. J. Elliott and A. F. Gibson, "An Introduction to Solid State Physics and Its Applications", The Macmillan Press LTD London, (1982).

[22] L. Neel, Ann, Phys, 3, 137, (1948).

[23] Howard Anton, "Calculus with Analysis Geometry", John Wiely and Sons, (1984).

[24] V. R. Kulkarani , M. M. Todhar , A. S. Vaingankar , Ind. J. Pure Appl. Phys. 24, 294,(1986)

[25] N. Rezlesus , E. Rezlesus , Phys. Stat. Sol.,23, 2, 575-582 (1974)

[26] B. L . Patil, S. R. Sawant, S. A . Patil and R. N. Patil, J. Mat. Sci.,29,(1994).

[27] E. J. W. Verwey and J. H. De Boer. Rcc . Trav , Chim Pays Bas, 55 ,(1936).

[28] S. A. Mazen, A. A. Ghani and A. H. Ashotr, Phys. Stat. Sol. ,88, (1985).

[29] Hsin-Fung Cheng, J.Appl. Phys. , 6,56, (1984).

[30] L. G. Van Uitert, J. of Chem. and Phys. , 24, 1294, (1956).

[31] M. I. Klinger, J. Phys. C, 8, 3595, (1975).

[32] M. I. Klinger, Phys. Status Sol. (B), 9,79, (1977).

[33] D. Ravinder and K. Latha, Mat. Lett. ,247-253, (1999).

[34] A. Eatah, A. A. Ghni and E. ELFaram. Awy. Phys. Stat. Sol.(1988).

[35] Mbhagavantha Reddy and P. Venugopal Reddy . Phys. P. ,24, (1991).

[36] E. Blechstein, Physik. Z. ,39, 212, (1938).

[37] F. W. B rockman and P. H. Douling, Phys. Rev. ,77-85, (1950).

[38] J. L. Snoek, New Dadepments in Ferromagnetic Materials, Elsevier Company York, (1947).

[39] G. G. Koop, Phys. Rev. , 83, 121, (1951).

[40] G. Moitgen, Z. Angew. Phys. ,4, 216, (1952).

[41] J. Nwanje, J. Phys. (1980).

[42] B. Tareev, " Physics of Dielectric Materials ", C.M. Publishers M bscow, (1975).

[43] B. K. Kuanr, P. K. Sigh, P. Kishan and N. Kumar, S. L. N.Rao, Prabhat, K. Sngh and G. P. Sivastava, .Appl. Phys.,8, 63, (1988).

[44] D. Raviner and Kvijaya, Kumar. Bull. Mater. Sci. ,24, 5, 505-509 (2001).

[45] B.P. Jacob,S.Thankachan,Sh.Xavier,J.Alloys.Compd., 578,314-319. (2013)

[46] S.A.Mazen,Mat.Chem.and Phys., 62,139-147,(2000)

[47] A.M.El-Sayed,Ceramic International.,28,363-367,(2002)

[48] C. Upadhyay, H. C. Verma, C. Rath, K. K. Sahu, S. Anand, R. P. Das and N. C. Mishra, J. of Alloys and Compounds, 326, (2001).

[49] S. A. Jadhav, J. Mat. Sci. Lett. , 224, 167-172, (2001).

[50] D.Ravinder,A.V.Ramana Reddy,Mat.Lett.,38,265-269,(1999)

[51] U. Ghazanfar, S.A. Siddiqi , G. Abbas. Mate. Scie. Engi.(B),118, 132-134,(2005)

[52]El-Shabasy , J. Magn. Magn.Mat., 172, 1, 188-192,(1997)

[53] B. Ravikumar and D. Ravinder, Mat. Lett., 53, 437-440, (2002).

[54]   P.A. Jadhav, J. Phys. Chem. Sol., 70, 2, 396-400,(2009)

[55] J. Azadmanjiri .Mate. Chem. Phys., 109, 109–112, (2008)

[56] L. S. Collectt and T. S. Katsubel, Geophs, 38, 76, (1973).

[57] J. S. Dugdal. ” The Electric Properties of Metals and Alloya”, Edward Arnold, (1977).

[58] P. V. Reddy and M. Salagram, Phys. Stat. Sol. (A) ,100, 639, (1987).

[59] S. A. Patil, S. M. Otarl, V. C. Mahajan, M. G. Patil, A. B. Patll, N. K. Soudagav, B. L. Patll and S. R. Sawant, Sol. Stat. Comm. , 78, 1, 39-42.8, (1991).

[60] R. D. Waldron, Phys. Rev., 99, 1717, (1955).

[61] S. T. Hanfner, Z. Krist, 155, 331, (1961).

[62] R. S. Patil, S. V. Kakatkar, A. M. Sanlepal, S. R. Sawant, J.Pure Appl. Phys.,2,193, (1994).

[63] S. A. Mazen, M. H. Abed Allah, R. I. Nakhla and H. M. Zaki. Mat. Chem. Phys. ,34, 35-40, (1993).

[64] S. A. Mazen, N. A. Hakeem and B. A. Sabrah, Phys. Status Sol. (b), KI,123, (1984).

[65] A. M. Shaikh, S. A. Jadhav, S. C. Watawe and B. K. Chongnle, Mat. Sci. lett.,44,192-196, (2000).

[66] B. J. Evans and S. Hanfner, J. of Chem.and Phys., Sol. ,29,1573, (1968).

[67] B. Vishwanathan and V. R. K. Murthy. ” Ferrites Materials ”, .Sci. Technol.,6-7, (1990).

[68] Xioa-Xia Tang, A. Manthiram and J. B. Good-enough, J. Sol. State Chem.,79, 250-262, (1989).

[69] S. S. Belled, R. B. Pujar and B. K. Chougule, Mat. Chem. Phys. , 52,166-69, (1998).

[70] V. A. Potakova, N. D. Zvera and V. P. Romanov, Phys. Stat. Sol. (A) ,12, 623, (1972).

[71] K. J. Standly, ” Oxide Magnetic Materials ”, Clarendon Press Oxford, (1972).

[72] A. A. Sattar, Phys. Solid Sta., 171, 563, (1999)

[73] S. H. Patil, S. I .Patil, S. M. Kadam, S. R. Patil, B. K. Chougule and Bull Mater Sci. 14 ,5, 542-545, (1991).

[74] R. S. Patil, P. K. Masker, S. V. Kakatker. S. R. Jadhav, S. A. Patil and S. R. Sawant, J. Magn. Magn. Mat., 102, 51-55, (1991).

[75] J. Smit and H. D. I. Wijin. Les Ferrites. Paris. Douod, (1960).

[76] S. A. Mazen and H. A. Dawoud, Phys. Stat. Sol. (A) ,172, 275, (1999).

[77] R. G. Kulharni and V. U. Patil, Mater, Sci. ,17, 843 ,(1972).

[78] Y. Yaff and C. Kittel, Phys. Rev. ,87- 90, 290-295, (1952).

[79] C. N. Chinnassamy, A. Narayanaasmy, N. Poupandian and K.Chattopadhyay, Mat. Sci. Eng. A, 04-306, (2001).

[80] A. L. Eatah, A. A. Ghani and M. F. El-Shahat, Phys. State Sol. ,104, 793, (1987).

[81] A. T. Eatah, A. A. Ghani and E. E. Earanaway, Phys. State Sol.(A), 105, 231,(1988).

[82] S. H. Patil, S. I. Patil, S. M. Kadam and B. K. Chougule,222 Czexh. J. Phys.Czechoslovakial, 42, 939, (1992).

[83] Rabinkin LI, Novikova ZI. Ferrites.Minsk,146,(1960)

[84]Pal M,Brahma P, chakravorthy D.j Magn Mater 152:370,(1996)

[85] R. R. Heikes and W. D. Johnston, J.Chem. and Phys. , 26, 582, (1975).

[86]M.E.Shabasgy.J.Magn.Magn.,172,188-192(1997)

[87]Klinger MI. j phys stat sol., 79B:9(1977)

[88]K.V. Kumar, D. Ravinder, Int .J. Inor. Mater., 3661-666(2001)

[89]K. R. .Krishna, K.V.Kumar, D.Ravinder, Adv.Mater.Phys.Chem.,2,185-191(2012)

[90] D. Ravinder, Mat. Lett. ,43, 129-138, (2000).

[91] H. H. Joshi and R. G. Kulkarni, J. of Mat. Sci. , 21, 2138-2142, (1986).

[92] N. Rezelescu and C. R. Acad. Sci. Ser. B (France) ,270, 18, 1143, (1970).

[93] M. A. Gillfo. Phys. Rev, 109,777 ,(1958).

[94] H. Ismel, M. K. ELNimr, A. M. Abou ELAta, M. A. ELHiti and M. A. Ahmed.Magn. Magn. Mat. ,150, 403, (1995).

[95] M. A. EIHiti, M. A. Ahmed, M. M. Mosad and S. M. Attia, J. Magn. Magn.Mat., 150 , 399, (1995).

[96] S.Mahalakshmi , K.S. Manja, J. Alloys Compd., 457, 1-2,522-525(2008)

[97]V.R.Murthy , J.Sobbhandari, State Solid Physic A,36, 2, K133-K135 (1976)

[98] K. Iwauchi, J.Appl. Phys., 10, 1520-1528, (1971).